Multi-spectra Artificial Compound Eyes, Design, Fabrication and Applications

YAO, Yupei

A Thesis Submitted in Partial Fulfillment
of the Requirements for the Degree of
Master of Philosophy
in
Mechanical and Automation Engineering

The Chinese University of Hong Kong

September 2013

Thesis/Assessment Committee

Professor CHEN Shih Chi (Chair)

Professor DU Ruxu (Thesis Supervisor)

Professor WANG Xiaogang (Committee Member)

Professor Chen Y.H. (External Examiner)

Abstract

Low-cost high-performance imaging is changing the world. Presently, nearly all cellular phone, laptop computer and the tablet have one or more than one cameras. Moreover, customers are demanding more functions.

This thesis introduces a Multi-Spectra Artificial Compound Eyes (MSACE) imaging system. Such a system is widely adopted in the nature. For example, viewing with specific spectrum, a bee can find a flower miles away. Though, there is no such a system in the market. Existing technology includes artificial compound eye and multi-spectra filters, but not a combination of both. In the thesis, the details of making a MSACE imaging system is presented. First, multi-spectra optical filters are made using color pigments selective by means of selective photolithography. Next, micro lens arrays (artificial compound eye) are fabricated using a combination of photolithography and the thermal reflow. Based on experiment testing, it is seen that the presented MSACE imaging system has following features:

- It has an accurate lens profile and hence, can catch accurate images.
- Different lens sections can catch different spectral images, which may show the hidden patterns of the observing objects.
- It is inexpensive and hence, may have many potential applications, such as medical diagnosis, personal identification, and currency counterfeit checking.

摘要

低成本高素质的成像器已经让高清摄像头走进各种电子产品，如手机，笔记本电脑以至平板电脑，人们开始希望这些摄像头能有更多新的功能。

这项研究介绍了一种结合了多光谱滤光片的类似复眼结构的镜片组成像系统(MSACE)，现有相关研究只有关于利用人工复眼结构进行图像阵列成像，或者利用后期处理方式得到多光谱图像，而本研究旨在将人工复眼结构与多光谱滤镜结合，使多光谱成像能与人工复眼结构结合应用。其制造方法如下：先利用颜色光阻剂在基底上形成不同光谱的滤光区域，再在其上用光刻胶和热熔法形成镜片阵列（人工复眼结构）。这个多光谱人工复眼结构成像系统（MSACE）具有以下特点：

- 镜片表面曲线光滑；

- 不同滤光片区域的镜片能同时获取不同光谱的图像，可以此观测到目标物在特定光谱下才显现的隐含特征，或建立立体图像；

- 制造成本低廉，可用在医用内窥镜以及验钞机。

Acknowledgement

First of all, I would like to thanks my parents. Having been studying in Hong Kong since 2007, I spent very little time at home. Although I did not have much time with them, they always concerning about me every single day – about my study, my emotion, my livelihood. It was my bad to let them worrying about me so much and I really feel sorry about that. They even came to Hong Kong at my undergraduate graduation ceremony – they were very difficult to arrange time together – and I felt so warm but compunctions at the same time. I have to say thank you again for everything they do for me.

May I also express my big thanks to my supervisor, Prof. Ruxu Du, he gave me lots of ideas on my research, and always help me solve the challenges. On the other hand, I would also like to thanks Dr. Di Si, Mr. Jin Jian and Li Hua, Mrs. Chen Qiulan at GIAT (Guangzhou), they either provided ideas for me and willing to teach me how to carry out the research project, or shared their experience related to my research and point out what practical factors should be taken into consideration, without their help, my research can never achieve so far.

Finally, I want to thanks my friends who always support me either in office work or daily life. The all are the best treasures I gain in the Chinese University of Hong Kong.

Yao Yupei
June 2013

Table of Contents

Index of Figure

1. Introduction

1.1 Introduction to compound eyes

In nature, there are mainly two different types of imaging systems, one is composed of two single aperture eyes, called binocular imaging system; most of high-level species, such as fish, reptiles, birds or mammalian like our human beings, are using this type of imaging system. The other is the compound eye imaging system, most of the insects, like flies, spiders, bees, and etc. are using this system. Figure 1 shows a sample of nature compound eye.

(a)   (b)
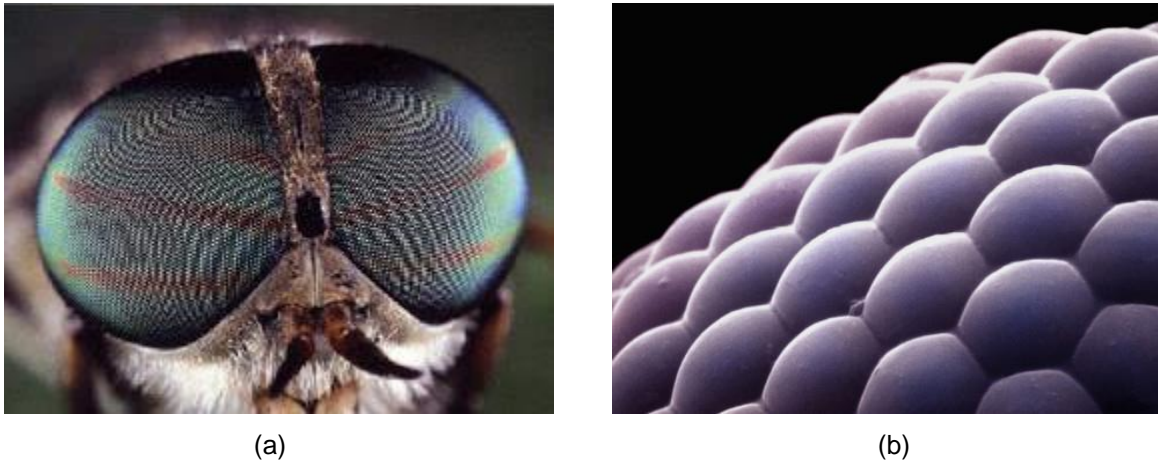
Figure 1: The compound eye imaging system [1], (a) overview of the whole compound eyes; (b) detail of the compound eyes

The compound eyes see the world differently, research shows that they cannot see things clearly, which means they may not have a focused vision, however, they have nearly 360 degree view and is very sensitive to motions [2]. A good example is

that one can hardly catch a fly, no matter which direction one tries to approach the fly and how slow or fast to move, the fly can always fly away just in time.

1.2 Artificial compound eyes

Inspired by the compound eyes in the nature, in the past few years the Artificial Compound Eyes (ACE) has becoming a hot research topic. The research includes to understand the nature compound eyes and to build artificial compound eyes. Although the nature compound eyes have many advantages like large view angle, sensitive to motion, etc., it has a major problem in building ACE: the focus function and mechanism cannot be built on a sphere surface. As a result, most ACE systems for imaging propose are built on flat surface, like the example shown in Figure 2, which can take the advantages of compound eyes, like taking multiple images at the same time, sensitive to motion, and etc.; and have the focus capability like the traditional single lens camera.

(a)   (b)
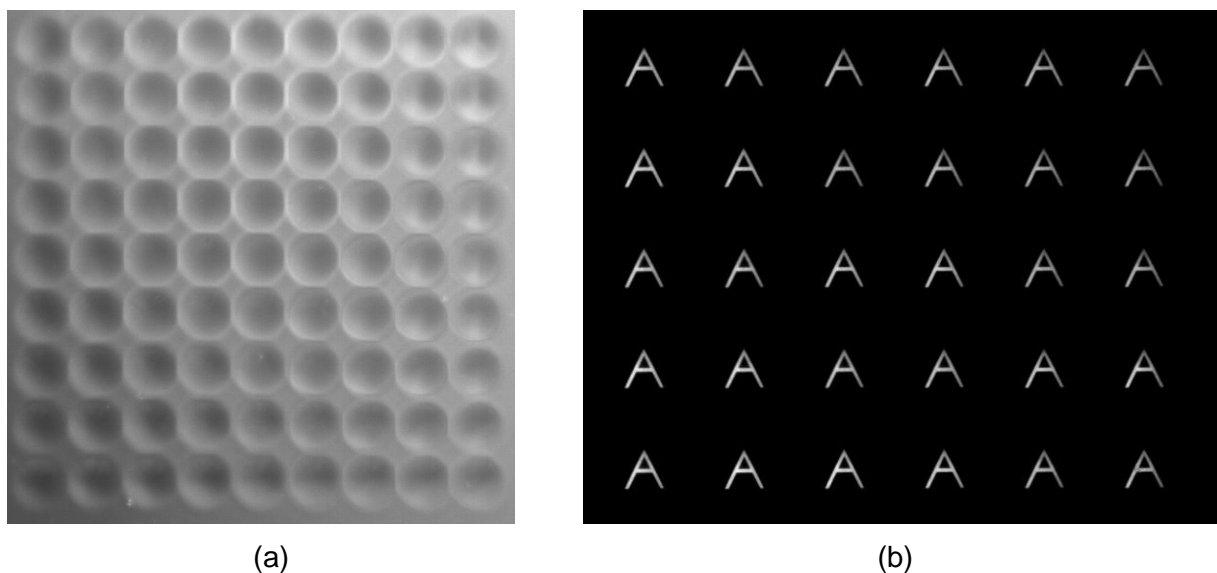
Figure 2: ACE structure (a) and sample imaging result (b) reported in [1]

1.3 Multi-spectra filter

Multi-spectra imaging has found many applications, such as satellites imaging and biological observation. As shown in Figure 3, multi-spectra satellite images can easily identify various kinds of land usage, such as urban region, forest, polluted water, etc. As shown in the figure, the lakes and different type of vegetation can be clearly seen.

Figure 3: A sample multi-spectral satellite imaging for land use identification [3]

Other application examples include currency counterfeit checking, special effect photography, infrared CCTV camera and etc. Figure 4 shows an interesting example: a flower has different views under normal photography and selected spectrum

photography. It seen that the two views are very different. In particularly, the selected spectrum (ultraviolet) image highlights the pollen to attract insects.

Figure 4: Common dandelion under visible and selected spectrum (ultraviolet) imaging [4]

1.4 The advantages and applications of multi-spectra artificial compound eyes

Combining the ACE and the multi-spectra filters, the Multi-Spectra Artificial Compound Eyes (MSACE) would have the advantages:

- Small in size: The lens element of a MSACE system can be made less than 1 mm while its imaging quality is still good;

- Large field of view: The MSACE system can achieve wide angle viewing without the concern of barrel distortion;

- Stereo vision: The MSACE system can easily provide sufficient information for stereo vision.

Because of the aforementioned advantages, the MSACE system could have many applications. A few examples are shown below:

- Medical diagnosis. The MSACE system can identify pathological tissues from normal tissues. In addition, its wide viewing range helps furnishing the endoscope inspection;

- Special effect photography. The MSACE system can conduct currency counterfeit checking, body temperature checking, and etc;

- Satellite imaging. The MSACE system can help to reduce the burden of, satellites imaging on different spectra and different viewing resolution.

1.5 The objectives of the research

The objectives of this research are (a) to design and fabricate a MSACE system and (b) to test the system by means of experiments. Please be noted that this research is not duplicating insect eyes. The rest of the thesis is organized as follows: Chapter 2 presents the design and fabrication procedure of ACE. Chapter 3 presents the design and fabrication procedure of multi-spectra filters. Chapter 4 presents the design and the fabrication of MSACE. Chapter 5 contains the experiment testing results. Finally, Chapter 6 contains the conclusions and future work.

2. Design and Fabrication of Artificial Compound Eyes (ACE)

In this chapter, the recent research and development of the Artificial Compound Eyes (ACE) is first reviewed. Then two different methods to fabricate ACE – the conventional method and the MEMS method, are presented. Experiment results are also included.

2.1 Literature review

It has attracted a number of research teams around the world and several experimental ACE systems with different structures and functions have been reported. For instance, Duparre *et al* developed two apposition ACE systems with planar structure and spherical structure in 2004 and 2007 [5, 6], respectively. They got the large field of view but low resolution of image. Tanida et al developed a planar ACE system with compact and simple structure as well as image reconstruction software in 2001 [7]. Its reconstructed image has higher resolution. Subsequently, they developed several applications, such as fingerprint capturing, multispectral imaging and color imaging [8-10].

From a physical point of view, ACE is made of a number of micro-lenses imaging an object simultaneously. This implies that ACE is an inherent stereo vision system. In principle, it is capable of extracting 3D information of an object and/or its position [11]. Following our previous work [12], a multiple-focus ACE imaging system is introduced to measure the displacement of moving objects in 2½D space. Comparing to the

conventional multiple-cameras Stereo Vision System (SVS), the system uses a micro-lens array with multiple-focus and a single CMOS array. The micro-lens array is fabricated on a transparent substrate by MEMS technique. The images from the ACE are captured by the CMOS array. Thus, the system is much smaller than that of the conventional SVS and the hardware cost is lower too. In addition, because the position of each micro-lens is pre-determined, the calibration process is not necessary. These advantages make the system attractive for some fields such as medical endoscopy and industrial endoscopy inspection [13, 14].

2.2. The fabrication of artificial compound eyes

2.2.1 Conventional method

As ACE structure is small in size and has short distance between each element, so it is very difficult to use glass as fabrication material [7], however, with the development on accuracy control of injection molding, many papers report that the micro lens array has very good qualities made by injection molding method, and PMMA and PC have the best qualities. [15]

As the injection mold lens array can be a good reference either on profile or imaging, so with the help of Prof. Sandy To from The Hong Kong Polytechnic University, a set of designed plastic ACE is made, as they have facilities to do precision injection molding, Figure 5 shows some samples they provided. After carefully selected the parameters (e.g. center distance, focus length, lens diameter, and etc.) of the injection mold ACE, the two designs are as Figure 6 shows:
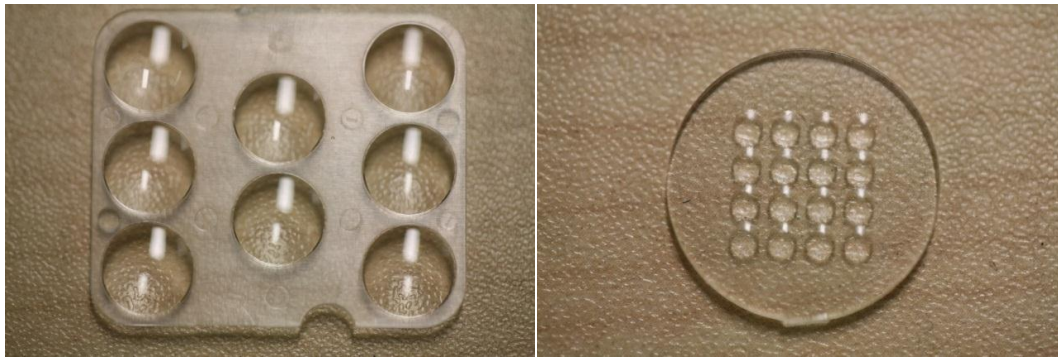
(a)   (b)

Figure 5: Samples of plastic optical lens array, (a) and (b)

Sub design #2

Substrate: 6.5mm diameter
Lens diameter: 1.5mm
Lens:
f=10mm, R=6mm, h=0.04706mm

Sub design #3

Substrate: 6.5mm diameter
Lens diameter: 1.5mm
Lens#1:
f=10mm, R= 6mm, h=0.04706mm

Lens#2:
f=5mm, R= 3mm, h=0.0952625mm

Lens#3:
f=15mm, R= 9mm, h=0.0313mm
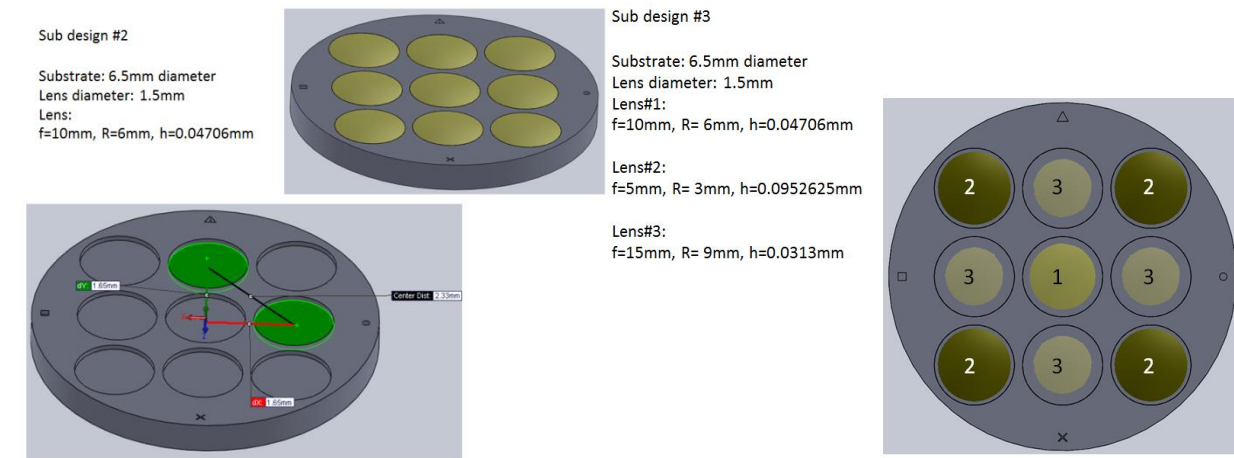
Figure 6: Two different design of ACE made by injection molding method

In Figure 7, the two designs of ACE is placed on the upper side, and the lowest one is the one made by mistake, however, from that one, it can be clearly seen that the substrate surface without lens pattern is frosting by design propose, which can reflect light and improve the imaging quality. Figure 8 shows the imaging result of this ACE made by injection molding.
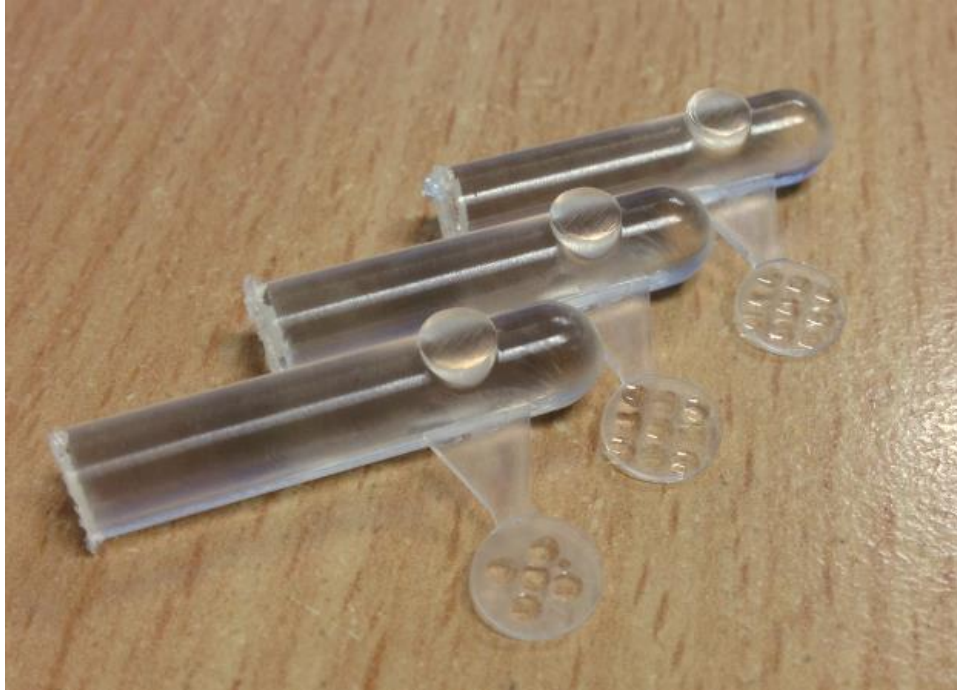
Figure 7: Sample of ACE made by injection molding method
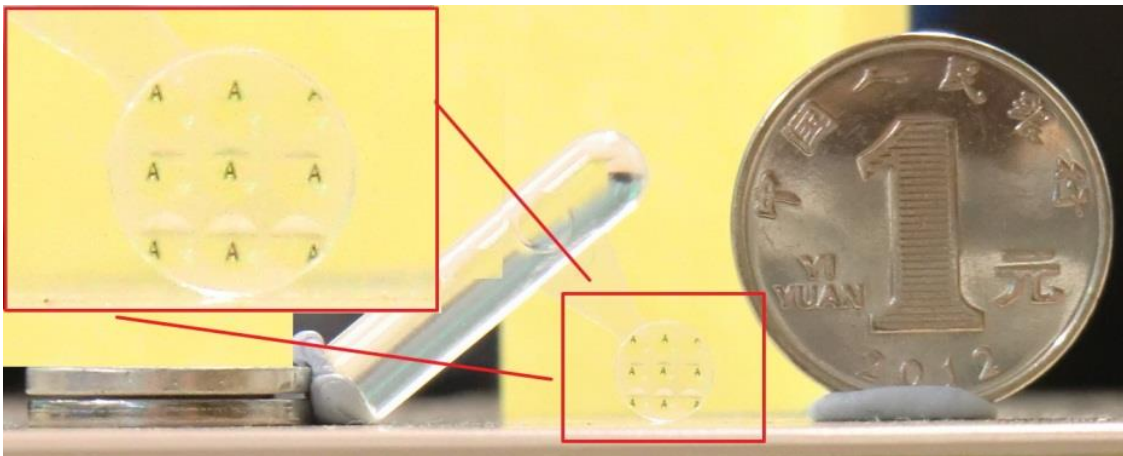
Figure 8: Image result of ACE made by conventional molding method

2.2.2 MEMS method

A micro lens array fabrication method that uses the photolithography technique and the thermal reflow method was reported by Di *et al* [16, 17, 18]. Their compound eyes imaging system contains a 9 x 9 microlens array on the planar glass substrate. As shown in Figure 9(a), the fabrication procedure can be divided into 3 steps. Firstly, the photo-resist layer is spin-coated on the substrate and then exposed by UV-light. Secondly, the photo-resist layer is developed forming a cylindrical isolated-islands array. Finally, heating the photo-resist islands until they melted will form spherical contour spontaneously because of the effect of surface tension.

(a)　　　　　　　　　　　　　　　　　(b)
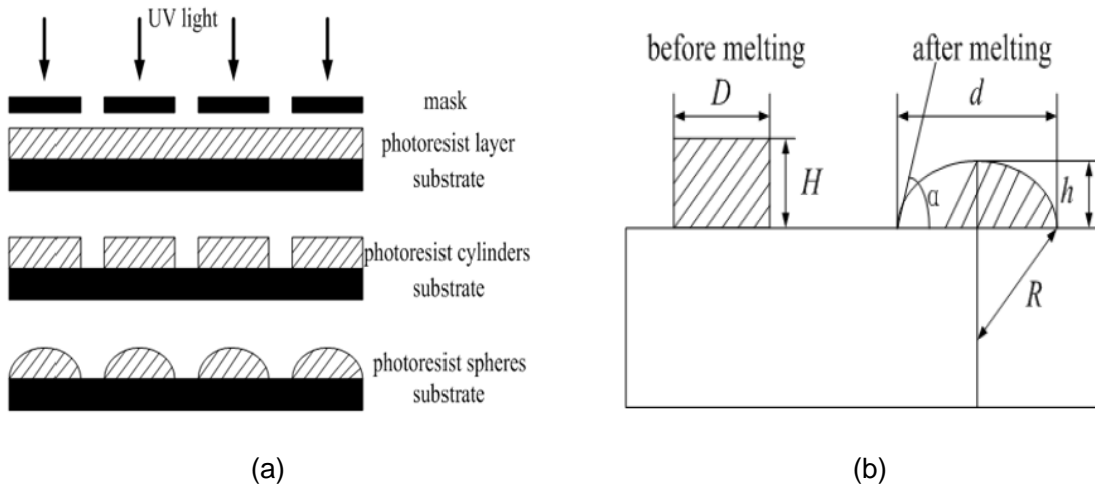
Figure 9: (a) AZ photoresist develop and thermal reflow general steps, (b) The key parameters in the thermal reflow [1].

In this research, a similar procedure is used. As shown in Figure 10, the detailed steps of fabricating the ACE are as follow:

Step 1:   Spin-coat the AZ 4620 photoresist on the substrate (1st run: spin speed = 400 rpm, time = 20 s; 2nd run: spin speed = 1000 rpm, time = 60 s);

Step 2:   Remove the residual solvent using pre-bake (temperature = 80 $^{\circ}$C, time = 2 min);

Step 3:   Repeat step 1 & 2 once;

Step 4:   Expose the photoresist with UV light under the cover of the prepared mask (exposure dose = 220 mJ);

Step 5:   Develop in the specific K-400 developer (K-400:Water = 1:4, develop time = 70 s), by which one section of the structure is formed.

Step 6:   Thermal reflow by the baker (temperature = 130 $^{\circ}$C,, time = 120 sec.).
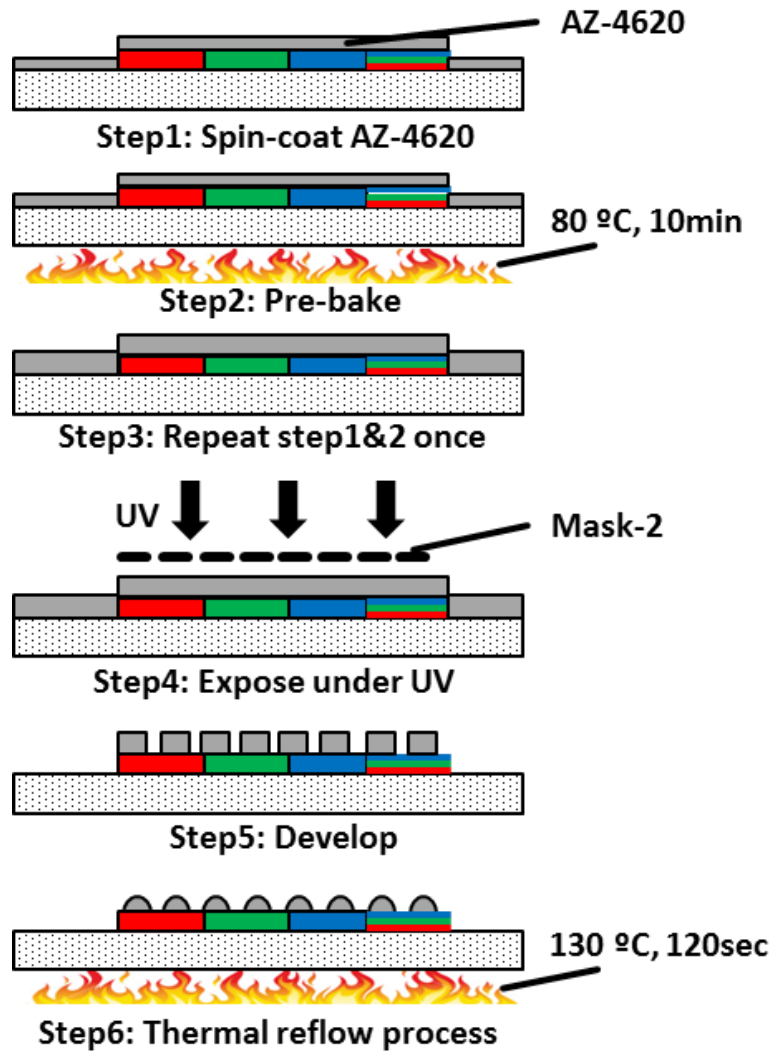
Figure 10: Procedure of making ACE using MEMS method with thermal reflow

Because different type substrate and facilities are used in the research, so the parameters from references may not be applicable, and because the thermal reflow process is not a standard process in photolithography, so some steps that are developed in the research need to be highlighted, otherwise prefect micro lens cannot be fabricated:

- A little bit "underdeveloped": not like normal photoresist operating procedure, the area outside pattern location cannot be fully develop during development process, it's because while doing thermal reflow, the pattern parts need transfer liquid state material from surrounding area to complete the reflow, otherwise the small pattern cannot reflow to the lens sharp as the surface tension between glass substrate and photoresist will stop it. Through experiments, 2-3 μm "underdeveloped" has the best result, after development, the test piece is look like what Figure 11 shows. There are two ways to do the underdeveloped effect: a little bit underexpose or manually controlled while doing the developing process, the first one is recommended, because the second one only has a few seconds proper "stop development" time, if missed, the photoresist will be fully developed, and needs to be cleanup and do it again.
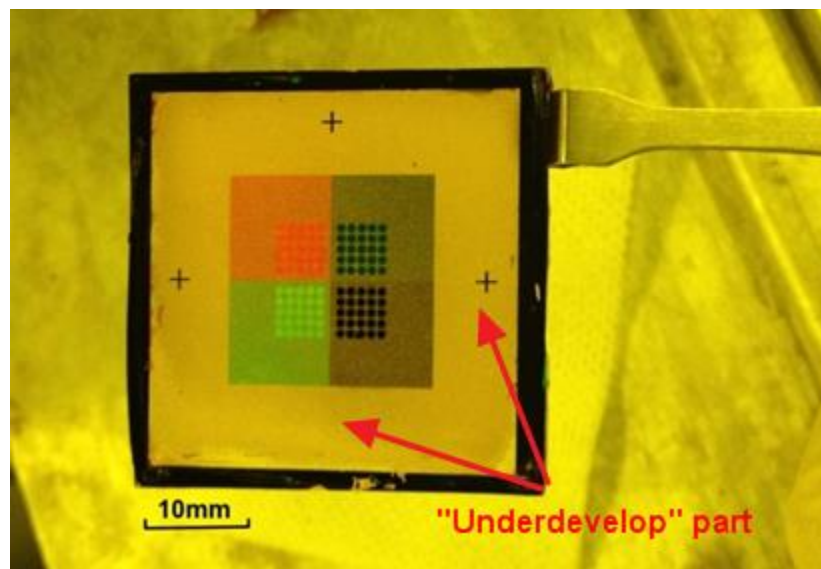
Figure 11: "Underdevelop" of photoresist.

- Thermal reflow time and temperature control: because every oven has its own temperature measurement unit, and different location in the oven may have different temperature, so the displayed temperature usually not the real values on the substrate. The way of solving this is use same location in the oven to bake, and temperature difference between soft-bake (baking after spin coating) and thermal reflow to find best combination of time and temperature. During experiment, it is found that +50℃ when doing thermal reflow with respect to soft-bake temperature has best reflow rate, so it is only needed to control the reflow time. As mentioned in first part, in the thermal reflow period, from the cylinder to a sphere surface, the section view will represent like a hump-like shape, which means the center point will rise to the highest point at last, the pilot process of section view is shown in Figure 12, from left to right

(a)　　　　　　　　　　　　(b)　　　　　　　　　　　　(c)
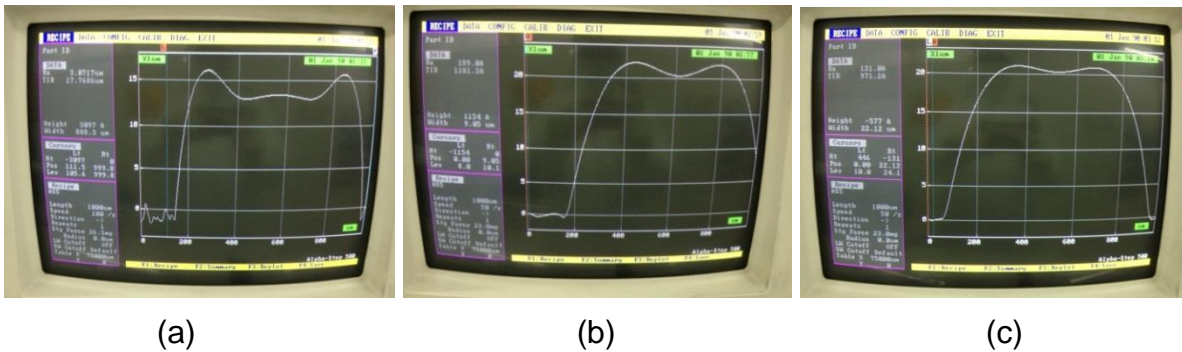
Figure 12: Pilot process of thermal reflow process (single lens section view)

- The photoresist coating is very thin, so bubblers is very annoying, especially very small bubblers, like Figure 13 shows, it occurs when dropping photoresist onto the substrate and before the spin-coating, and as the viscosity of photoresist is high, bubblers are not easy to self-destructive, and if someone punch or tear to

14

break it, it may cause more smaller bubblers around, even a tiny bubbler can cause heavy damage to the whole coating due the centrifugal force. The way to avoid bubblers is steady and continually deposits the photoresist onto the substrate at only one location; and if bubblers occurred, use dropper to suck it up instead of breaking it.
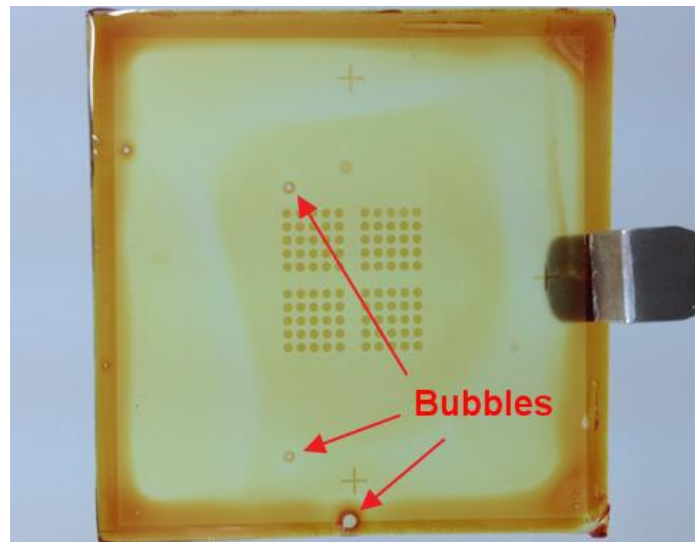
Figure 13: Bubbles in photolithography

- The coating thickness: for 700 μm diameter lens, the desired coating thickness is between 22 μm to 25 μm, too thin, the reflow cannot form lens, instead it will stop in one of the steps in figure 12 – has a hump-like section view, too thick, the lens array will join each other as there is too much material and has bad effect to the imaging quality, like the situation shows in Figure 14 (a) and (c).
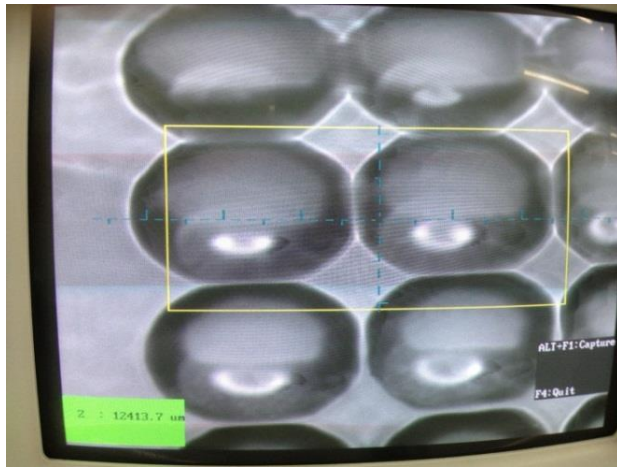
(a)
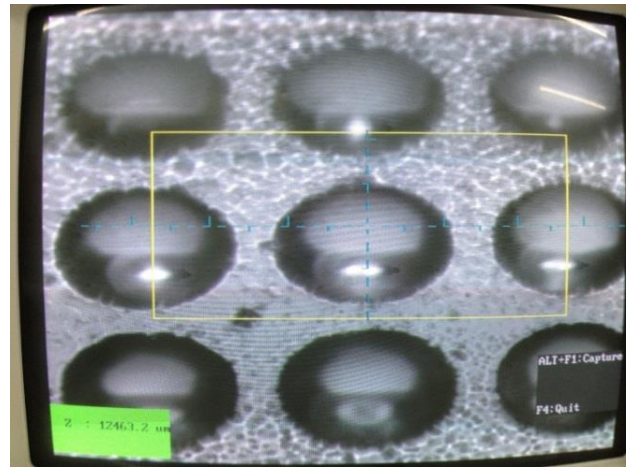
(b)
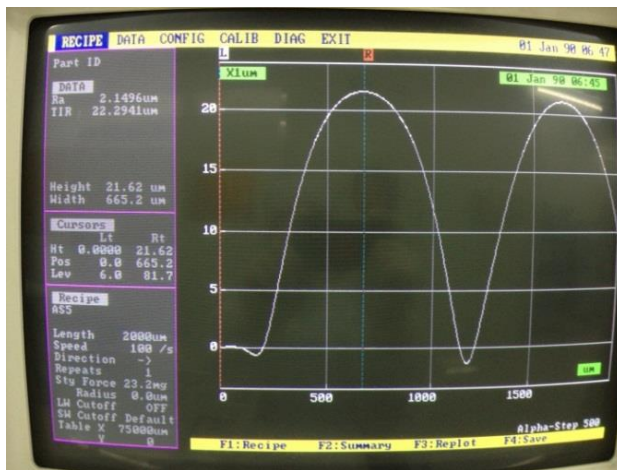
(c)
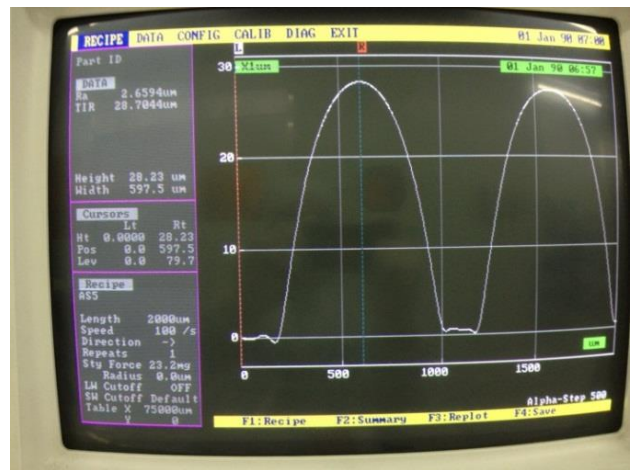
(d)

Figure 14: (a) Coating thickness too high to cause lens joining together after melting, (b) Good coating thickness control, (c) Surface profile with too thick coating, (d): Surface profile with good result

The completed ACE sample image is shown in Figure 15, thermal reflow artificial compound eyes structure:
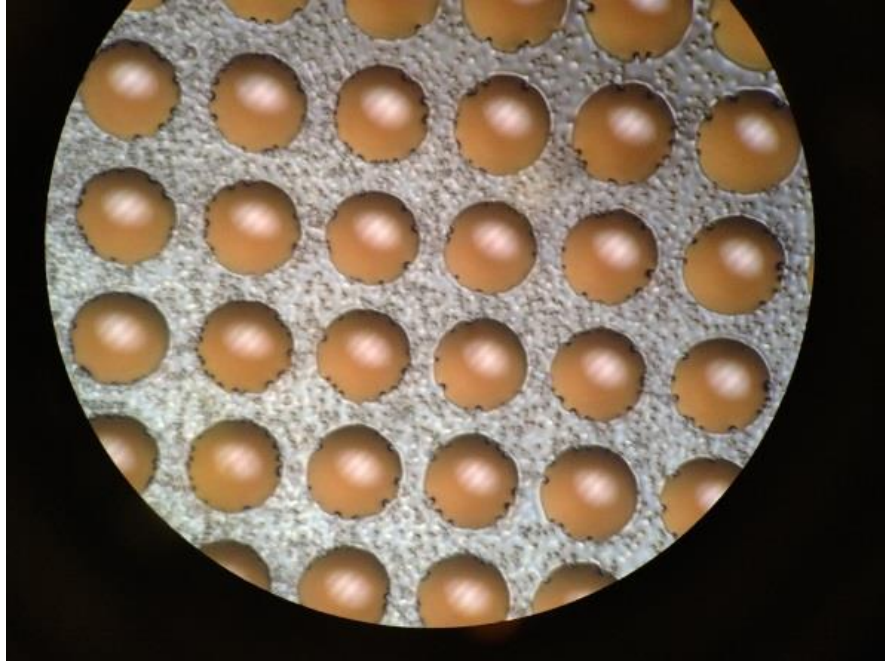
Figure 15: ACE made by thermal reflow method

3. Multi-Spectra Filters

This part shows the recent research and development of the multi-spectra filter, then introduce two different ways to fabricate multi-spectra filter – the multi-layer deposit method and the pigment based photoresist method. The pigment based photoresist method is included in the research to make the multi-spectra part of the MSACE.

3.1 Literature review

Optical filter coating technology has been developed for over a century, nevertheless, small, integrated and multi-spectra optical filter coating was only reported in the last decade, one of the latest advanced multi-spectra filter fabrication method was reported by Lin and Yu [18], in which a method named combined etching technique was presented by adjusting the thickness of space layer of F-P filter. In their research, a 16 channel micro integrated narrow band pass filter was fabricated within a small size substrate, whose feature size of unit filter width is 0. 7mm, relative half width of peak transmission is less than 1.0%, and peak position location accuracy is beneath 0.25%. The fabrication process is shown in Figure 16 (b)
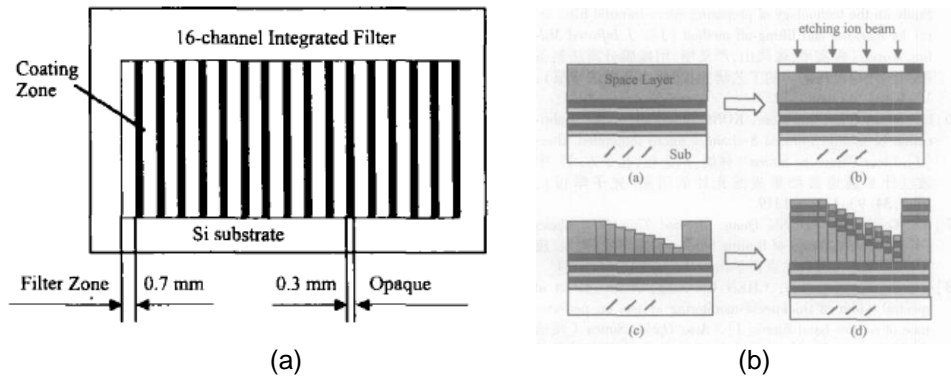
Figure 16: Fabrication of 16 Channel Micro Integrated Filters, (a) The mask for etching; (b) The fabrication process [18].

3.2 The fabrication of Multi-spectra filters

From literature review, the first idea of fabricating multi-spectra filters is using "additive" MEMS method to fabricate different and separate filters in restricted area. In order to have contrast to test the coating result, a set of commercial color filters are purchased, shown in Figure 17, most of them were custom made to 12 mm in diameter, which is easier to be mounted on the test platform.

Figure 17: purchased commercial color filters

As showed in the Figure 17, the purchased color filters contains 2 different kinds of Infrared pass filter, 2 kinds of UV pass filters, 2 different commercial level optical glass, (quartz and high quality white glass) and 5 kinds of other visible light spectra band-pass filters. (Filter spectra specification is attached in Appendix C) Most of them were custom made to 12mm in diameter, which fits the test camera lens' diameter for easier installation propose, the test platform setup is shown in Figure 18.

Figure 18: Setup of testing purchased color filter

Basically it is a simple system controlled by the computer using the R-145 port (LAN port). The setting is as follows: (a) Connect the camera to the computer; (b) Open the computer; (c) Open the Network and Sharing Center; (d) Select "Change adapter settings;" (e) Right click "Local Area Connection," (f) Select "Property;" (g) Double click "TCP/IPv4," (h) Select use fix IP: 192.168.1.2; sub mask: 255.255.255.0; gateway: 192.168.1.1; DNS: 192.168.1.1.

Because the camera has build-in software, it just needs to open an internet browser (e.g., Internet Explorer; Firefox; Chrome, etc.), then enter the URL: http://192.168.1.126:81, after the login process, the camera interface can be seen as shown in Figure 19:
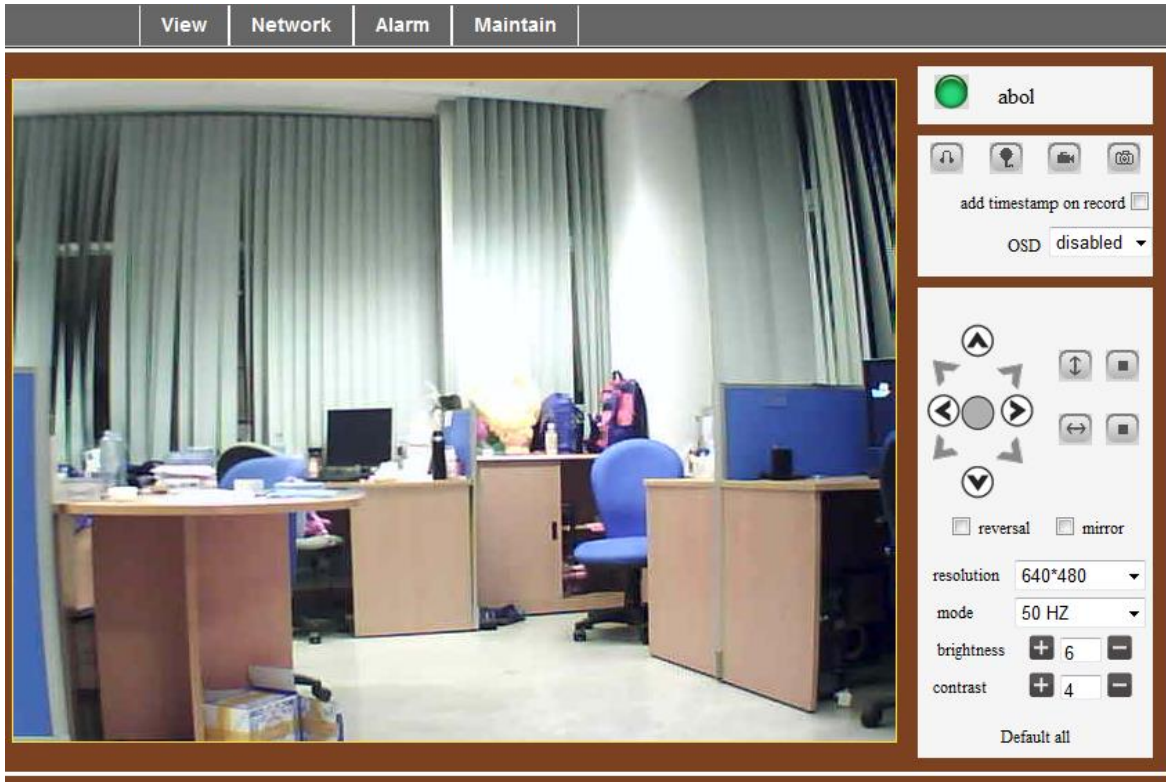
Figure 19: Interface of testing camera

A number of imaging results taken by the camera with and without color filters are shown below. Figure 20 shows the images without filters.

Figure 20: Original full spectra images

Figure 21 shows the images with the two blue filters, QB1 and QB4. From the figure, it is seen that QB1 allow more light to pass while QB4 allows mostly blue light to pass.

<div align="center">(a)   (b)</div>

Figure 21: Blue glass filter images, (a) QB1 result image; (b): QB4 result image

Figure 22 shows two Green/Yellow filter images. The JB470 just filter out spectra under 470nm, so it most likely seems like a normal image, except it loss some blue and violet color, CB535 filter out spectra under 535nm, without blue and violet light, so it looks yellow or green.

<center>(a)   (b)</center>

Figure 22: Green/Yellow glass filter images, (a) JB470 result image, (b): CB535 result image

Figure 23 shows the result images of two red glass filters. These filters only allow red lights or infrared pass though, the results shows some dark area in full spectra image change to different color because some components of the mixed color have been filter out. HB 630 allows most of the red light pass through, so the whole result images looks "red", and HB 700 keeps only a few visible red light of human eyes, that's why only a few red color is shown in the image, and other area keeps black and write.

<center>(a)   (b)</center>

Figure 23: Red glass filter images, (a) HB630 result images; (b) HB700 results images

Figure 24 shows the results images of HWB 830 infrared filter, (a) is taken in the day time while (b) is taken in night, with inherent infrared light source of the camera. Since HWB 830 allows only infrared light to pass, so only black and write shows in the images, compare the two result images, consider the illumination angle issue, the objects in the image almost have the same result.

(a)   (b)

Figure 24: Imaging results using HWB 830 filter, (a) taken in the day time, (b) taken in the night with self infrared lighting from the camera

In summary, the testing images show that different color filters could produce very different imaging results and hence, revealing different features of a same scene. This implies that multi-spectra imaging is useful. Moreover, integrating the multi-spectra filters would capture more information.

3.2.1 Multi-layer deposition method

In order to have specific designed filters, coating design software Essential Macleod is used to help generate possible solutions of spectra filters. Figure 25 shows the software interface.
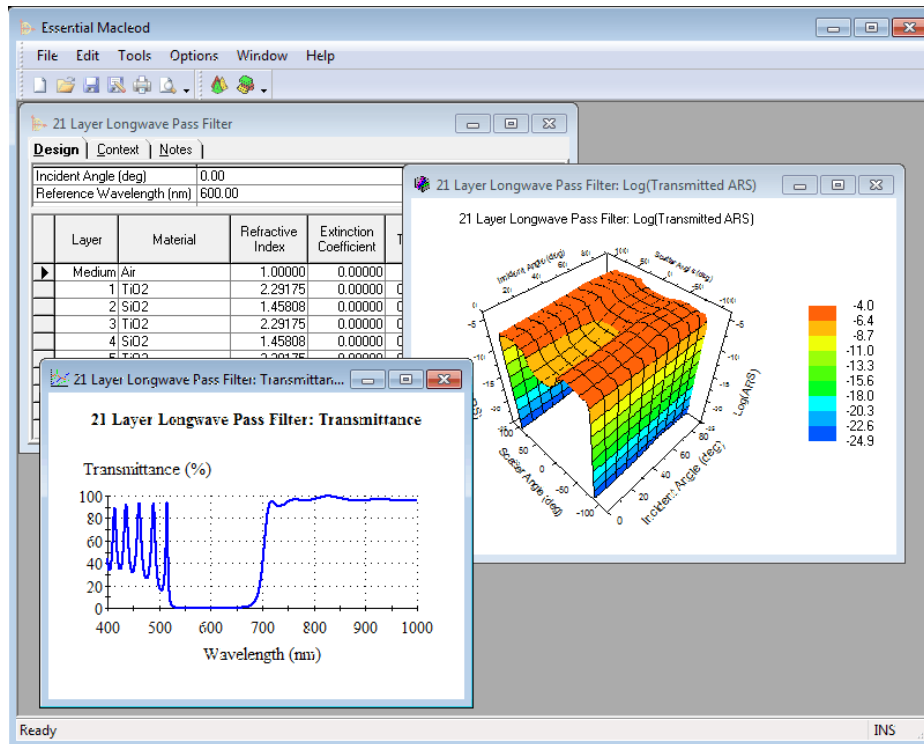
Figure 25: Filter design software interface

The design shows in Figure 26 is generated by the software. Though the transmittance is not very good, it is the best solution of using SiO2 and Si3N4 only. Some literatures suggest that using sputtering can improve [19].
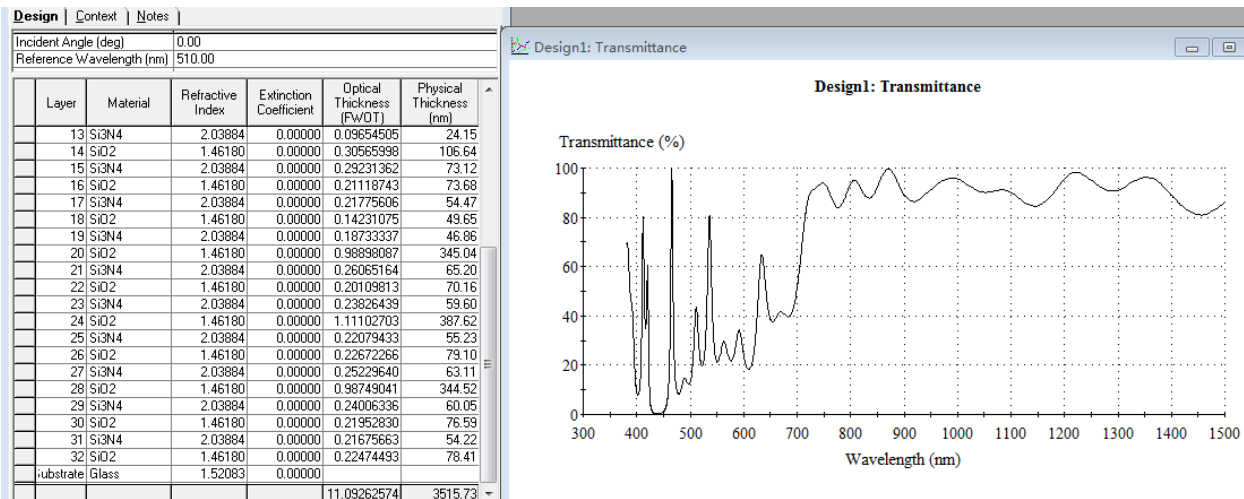
Figure 26: Multi-layer thin film filter designed by software

To test the transmittance, a simple setup is built as shown in Figure 27. The testing results are shown in Figures 28 and 29. From the figures, it is seen that the substrate sample with coating has even higher transmittance than the sample without coating. This implies the coating is failed.

Figure 27: Transmittance test setup of the first PECVD coating sample

Figure 28: Transmission rate curve of sample without coating
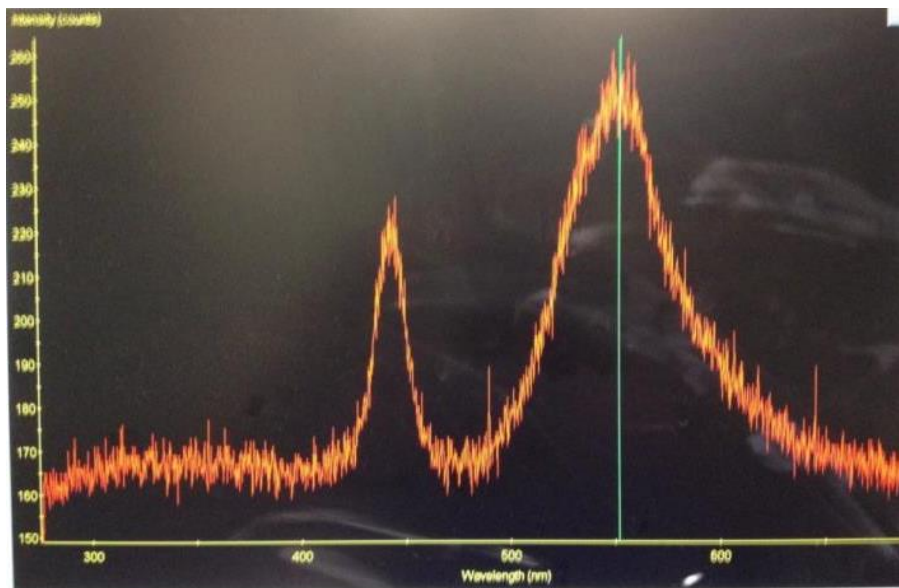
Figure 29: The transmission testing results of the PECVD coating

In order to find out the reason of the result, the substrate with coating was examined by electron microscopy. As shown in Figure 30, there are many light dots, which are probably generated instability of the process as discussed below.

Figure 30: Unexpected light dots on top of the surface of the substrate with coating

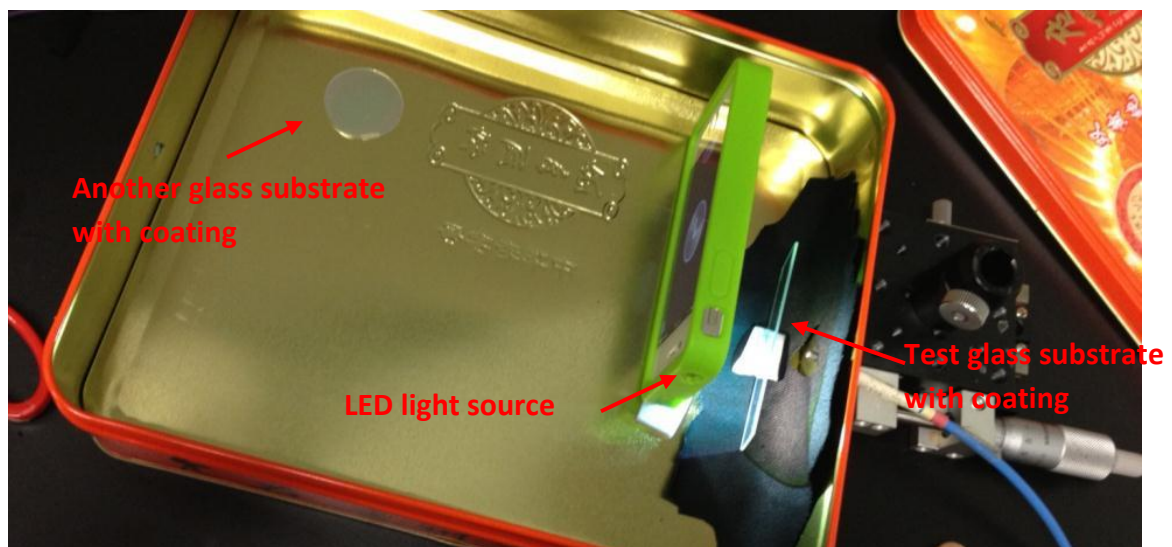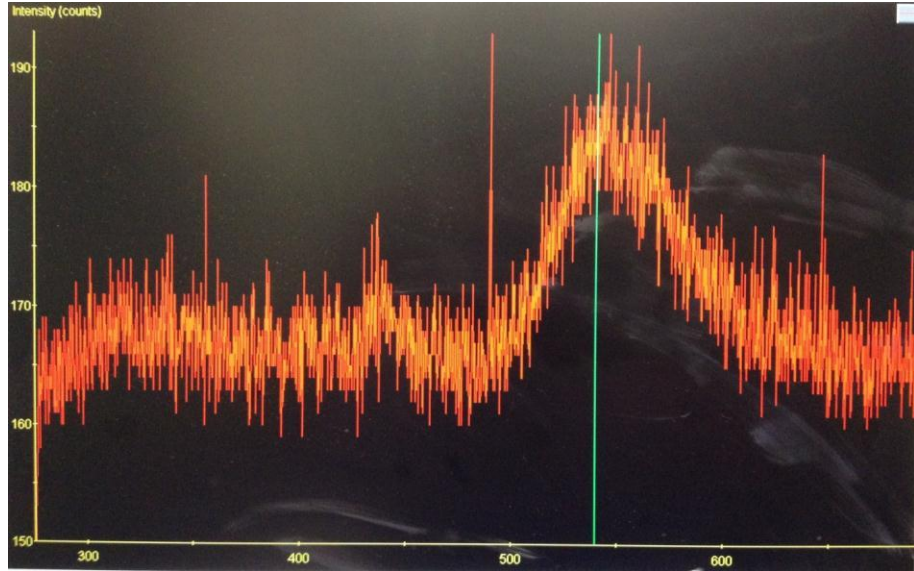To find out the reason of the light dot, the substrate was taken to use surface profiler to scan the surface, from Figure 31 and 32, the scan results show that that there are many bulges on the surface, which is the source of the light dot, this unexpected result may come from two reasons: one is that the substrate itself is inherently not flat enough, and the other reason is there is something wrong during the PECVD process – some literature infer that the precursor gas may cause the problem, the precursor gas setup in the clean room is designed for single lay deposit, while the design is multi-layer – 32 layers, so it may cause unexpected problems.
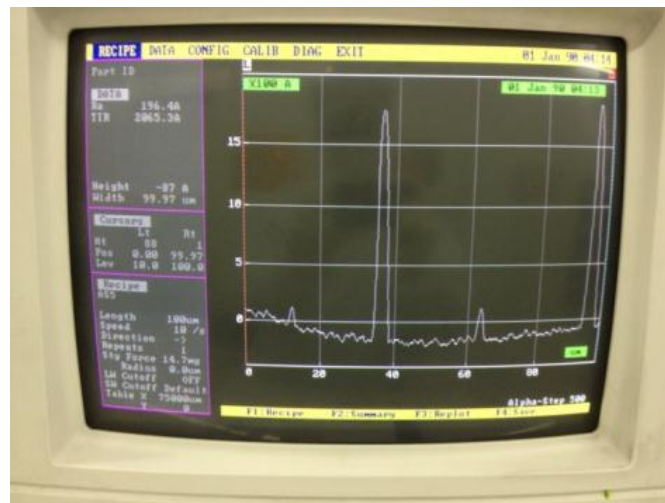
Figure 31: substrate surface profile scan – 100 µm length scan
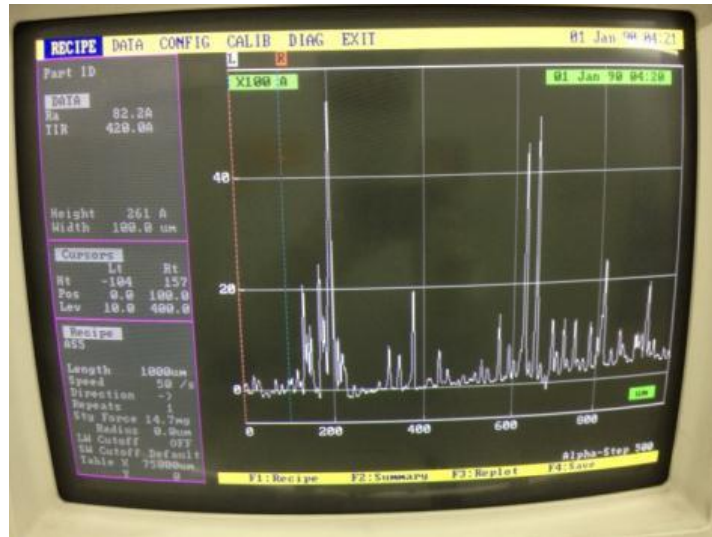
Figure 32: substrate surface profile scan – 1000 μm length scan

The solution about the problems can be: first, purchase high quality substrate, i.e. quartz glass or even mono-crystalline silicon glass, they will have better surface planeness; while the other problem is not easy to solve, because it's expensive to purchase new precursor gas, moreover, the parameter of PECVD machine in the clean room has been set, it take a lot of time to adjust new parameters for the new precursor gas, and at last, it cannot be 100% sure that changing new precursor gas can fix the problem, or it may cause new problems.

As a result, this method is not suitable for fabricating the multi-spectra filters – due to the limitation of facilities.

3.2.2 Pigment based photoresist method

In this research, the pigment-based photoresist material and photolithography technique is adopted [20, 21]. This technique is normally used in Liquid Crystal Display (LCD) manufacturing. A sample is shown in Figure 33. The pigment based photoresist materials are purchased from KEIRAKU Optical-Electronic Co. [22], the sample is made by photolithography.

Figure 33: Pigment-based photoresist sample on slides without any pattern

The pigment-based photoresist material is negative photoresist, which means the part that expose to the UV light will not be developed by its developer (KOH1001, 1: 49(water)), and permanently solidify after the hard barking, that means more color can be developed beside the successfully made color sections. Generally procedures of fabricating a color filter matrix with different pigment-based photoresists are shown in Figure 34.

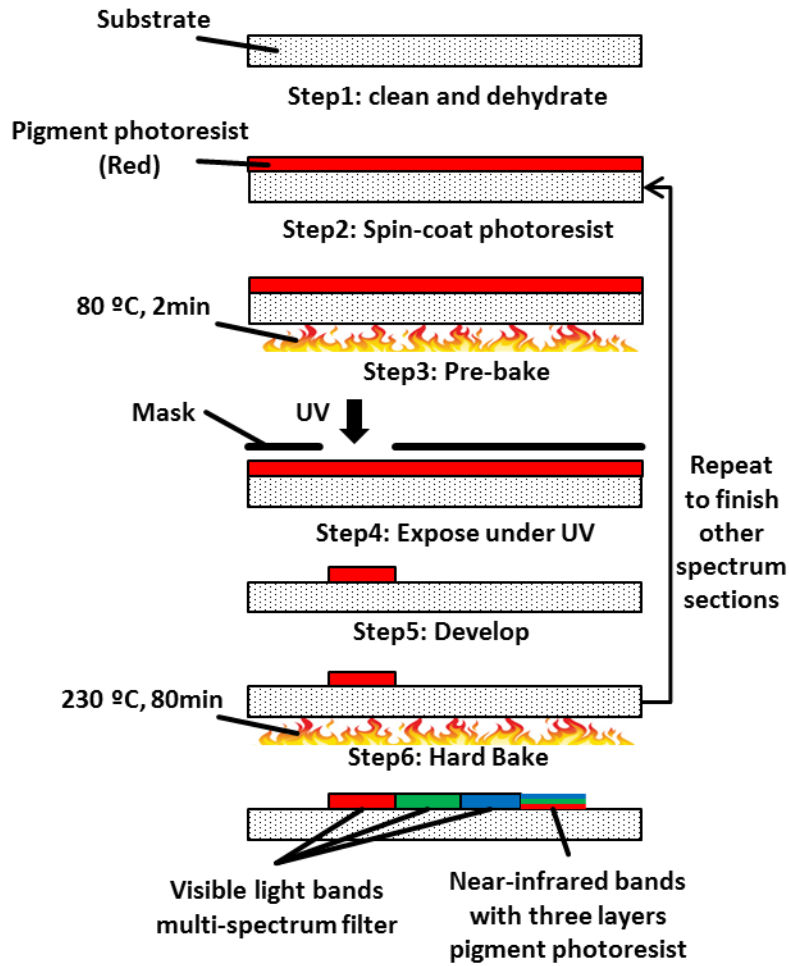Figure 34: procedure of color filter matrix fabricate by Pigment-based photoresist

The detailed steps of fabricate the color filter matrix are as follow:

Step 1:   Clean the glass substrate using acetone and dehydrate the substrate in the oven;

Step 2:   Spin-coat the pigment photoresist on the substrate (1st run: spin speed = 300 rpm, time = 20 s; 2nd run: spin speed = 600 rpm, time = 60 s, final thickness = 1 μm);

Step 3:   Remove the residual solvent using pre-bake (temperature = 80 ^{o}C, time =

2 min);

Step 4:   Expose the photoresist with UV light under the cover of the prepared mask

(exposure dose = 150 mJ);

Step 5:   Develop in the specific KOH developer (KOH:Water = 1:49, develop time

= 40 s), by which one section of the filter is formed.

Step 6:   Cure the photoresist completely using hard bake (temperature = 230 oC,

time = 80 min).

Using the aforementioned technique, two types of multi-spectra filters are made, one with four colors and the other with nine colors. The mask of fabricating the four-color filter is designed as shown in Figure 35. Note that during the fabrication, each time when fabricating a new color on the substrate, the alignment must be carefully taken to avoid overlap. A successfully fabricated four-color filter is shown in Figure 36.
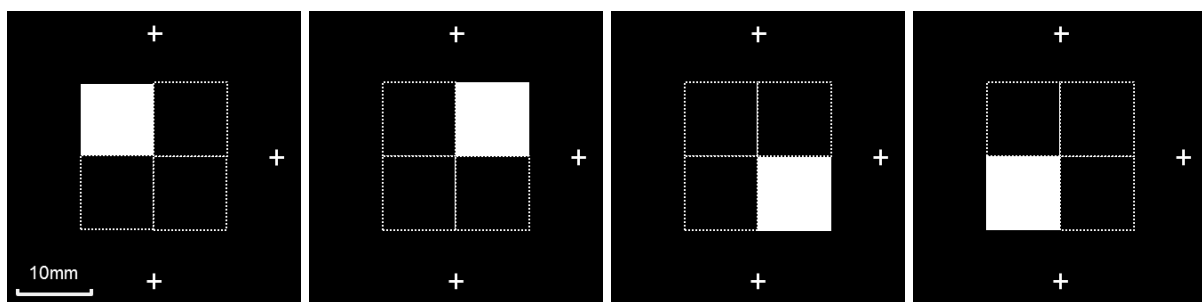
Figure 35: The 2 × 2 matrix masks for making the four-color filter (the dash line is for reference only and is not appeared in real masks)
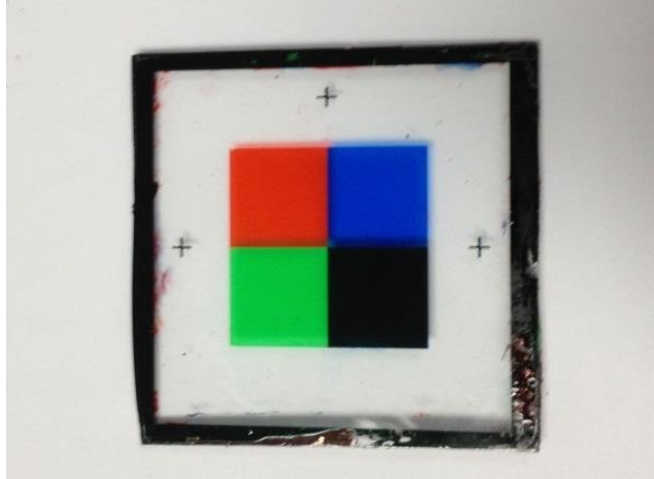
Figure 36: A sample 2 × 2 multi-spectra color filter

Next, the nine-color filter is made. As shown in Figure 37, it has 3 × 3 sections including 3 basic colors and 4 new colors: orange, cyan, yellow and violet (made by mixing the 3 basic colors), a blank section, as well as an infrared section (made by a combination of three basic colors overlapping together).

Figure 37: A sample of nine-color multi-spectra filter

In order to test the quality of the filters, quartz-halogen lamp is used as light source, and using spectrometer to measure the transmission rate, the formula is:

$$Transmission\ rate\ (\%) = \frac{result\ value\ passing\ through\ filter - background\ value}{result\ vlaue\ without\ any\ filter - background\ value}$$

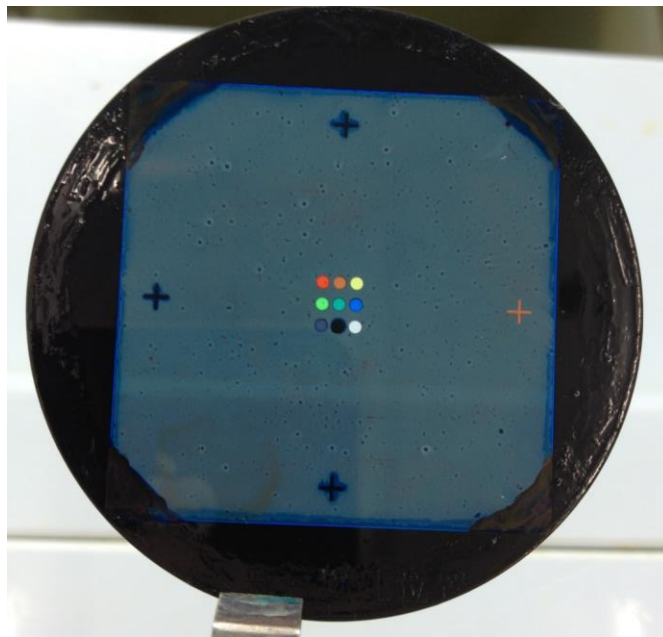The transmission rates of the four-color multi-spectra filter and the nine-color multi-spectra filter are shown in Figures 38 and 39 respectively. Note that the transmission rates of the three basic colors in the nine-color multi-spectra filter are the same as that of the four-color multi-spectra filter and hence, are not shown in Figure 39.

From Figure 38, it is seen that the three basic color photoresist have good band pass filter effects. Moreover, when the three basic colors overlap together, the combination has good infrared high-pass filter effect, which means almost all lights less than 800 nm is blocked.

From Figure 39, the yellow filter has the best result; the cyan and orange filters can provide some band-pass effects; and the violet filter gives only of poor 40% transmittance, which may be attributed to the light source containing little violet light.
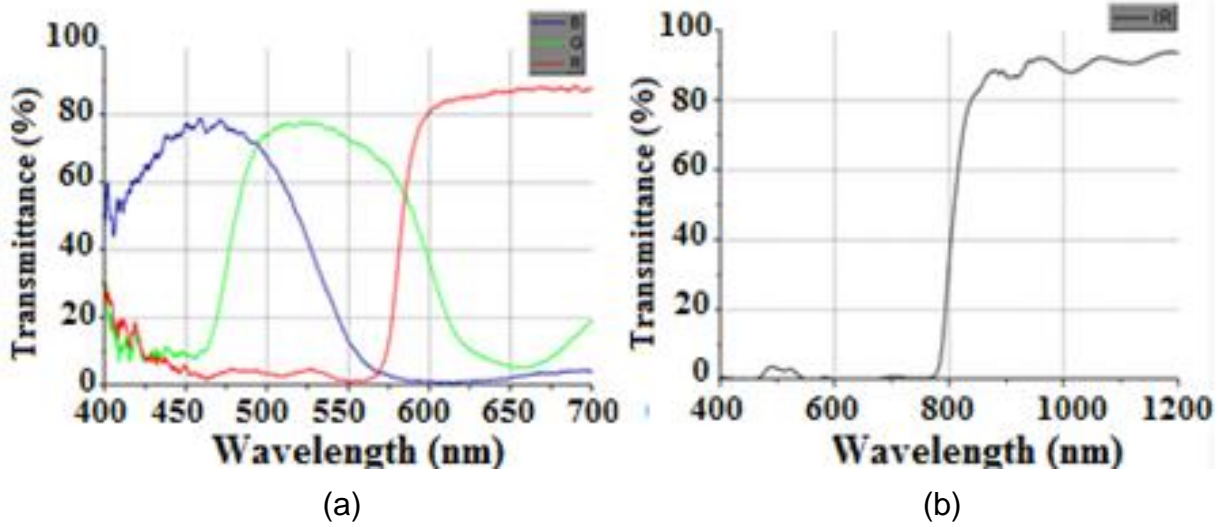
Figure 38: (a) Transmittance of the 3 basic color pigment-based photoresist, (b) the transmittance of the combination section of all 3 basic colors.
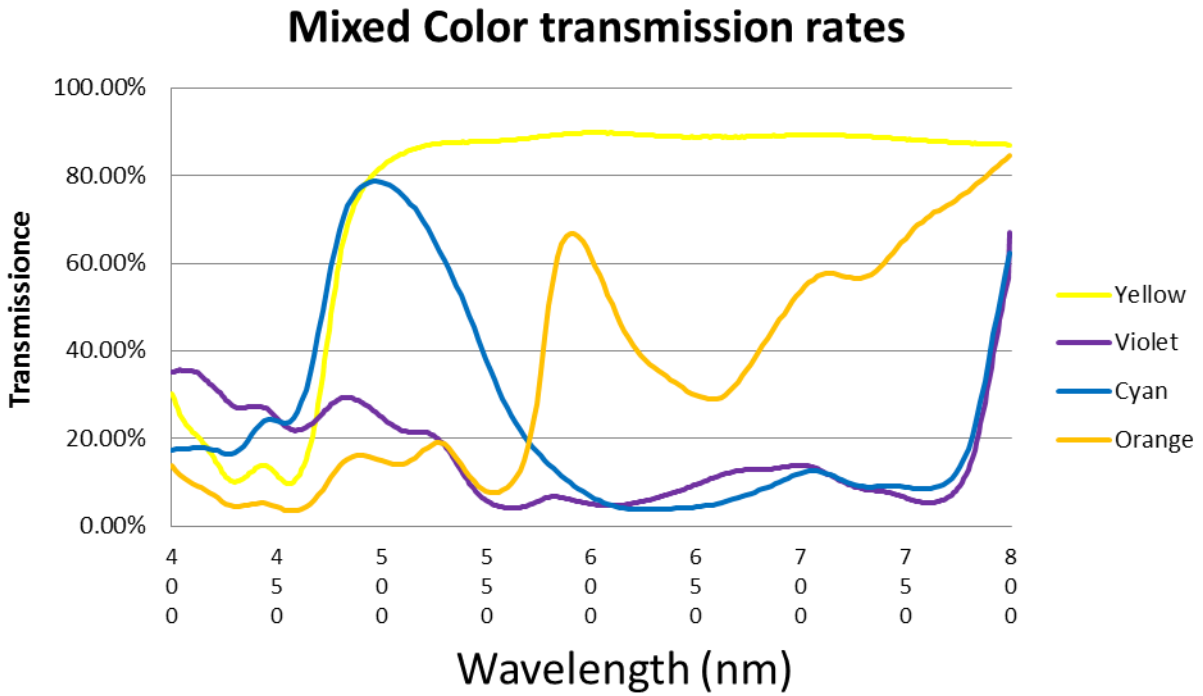

Figure 39: Transmittance rate 4 mixed color from 3 basic pigment-based photoresist

4. Multi-spectra Artificial Compound Eyes

To combine the multi-spectra filters together with Artificial Compound Eyes, there are some problems to solve, such as the procedures – which process should be done first, and how to protect the finished part when doing the subsequent part.

At the very beginning, the idea of combine these two parts is using physical method – digging a groove in one sample and embed another one into it, however the problem is obvious: there are not suitable tools to do the operation, and even the groove is successfully made, to keep two samples sticking together, glue is need, no matter which type of glue, it will add additional condition between two samples, the caused effects are uncertain, so this idea is abandoned. The goal is finding a method to combine two parts without any other material.

After careful review the property of two kinds of photoresist, a possible procedure of fabricating two parts on the same substrate is found: because the hard bake temperature of pigment-based photoresist is higher than the thermal reflow temperature, and the chemical properties of negative photoresist (pigment-based photoresist) become very stable after hard bake, so it's possible to fabricate the photoresist ACE on top of the Multi-spectra filters.

Through experiments, two problems found in fabrication by this method: First is the mask, since two different type of photoresist (positive AZ serious for thermal reflow and negative pigment-based for Multi-spectra filters) are used during the process, so the alignment marks on the mask need to be redesign, otherwise the mark will be

invisible when changing the photoresist material. The other problem is the flatness of the substrate is different when the Multi-spectra filter is finished, some area will have more than one layer pigment based photoresist, which means there will be several microns higher than other area, and the resulting problem is the remaining layer of positive photoresist for smoothly thermal reflow process – mentioned previously. The solution the second problem is slow down the spin-coat speed a little bit, in order to have thicker layers of positive photoresist, and that can keep the exposure time and develop time unchanged, to have thicker remaining layer, which to ensure that all area on the Multi-spectra filter have at least 1 μm thick remaining positive photoresist layer. After the two problems are solved, the MSACE was finally made, as shown in Figure 40. Same method can be also applied to make the 9 colors MSACE, shows in Figure 41.
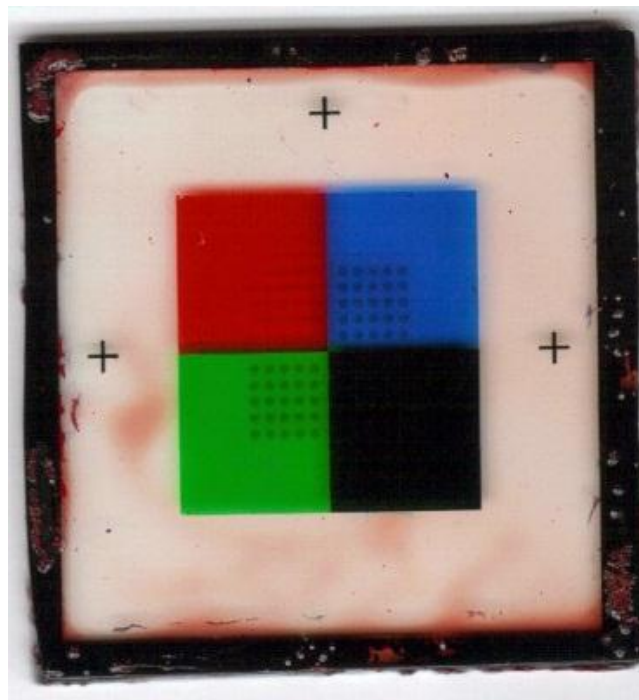
Figure 40: 4 colors MSACE
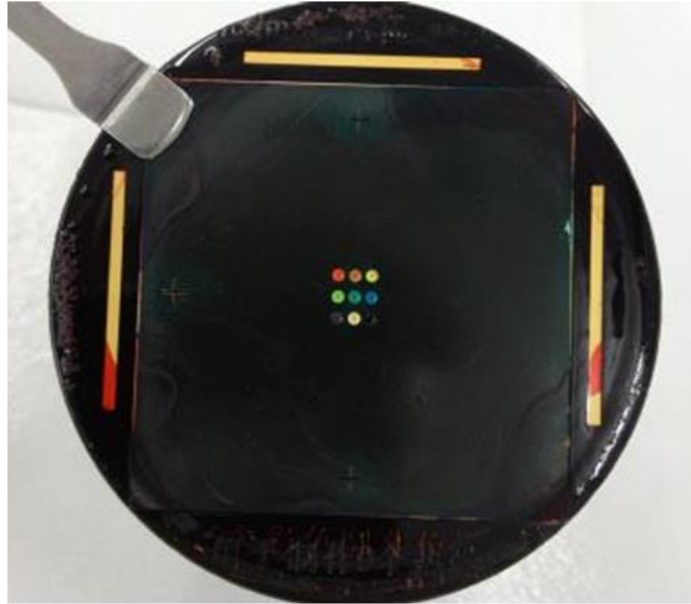
Figure 41: 9 colors MSACE (From left to right, up to down: red, orange, yellow, green, cyan, blue, violet, blank section and infrared pass)

Figure 42 shows the MSACE surface profile image taken by microscope with an amplification of 5 times, (a) is taken under background lighting while (b) is taken under normal lighting, from (a), the figure clearly shows the boundaries of different lens elements are continue and circular, from (b), the lines on the lens elements are the reflection of the normal lighting, and their evenly distribution means that the surface of the lens elements are smooth and spherical.

(a)   (b)

Figure 42: The center portion of 4 colors MSACE sample with an amplification of 5 times, (a) is taken under background lighting, (b) is taken under normal lighting
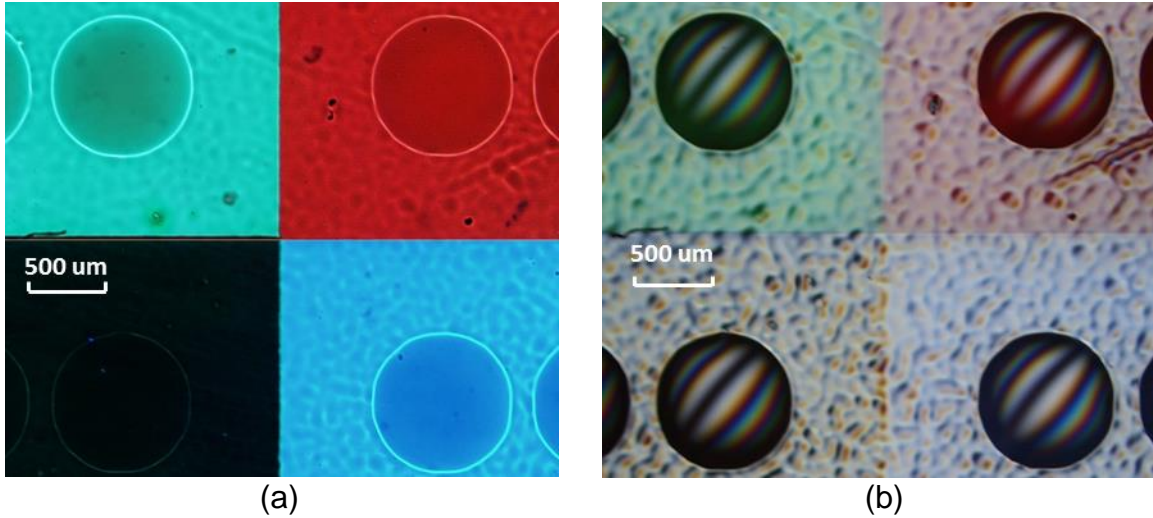
In order to validate the fabricated lens profile, a number of tests are conducted using Alpha-step 500 surface profiler. The results are showing Figure 43. From the figure, it is seen that the profile are very close to the designed surface. In particular, Table 1 shows the errors in percentage. It is clear that the maximum percentage error is less than 3%.

Section (a)	0.48%	Section (b)	2.15%	Section (c)	1.89%
Section (d)	2.26%	Section (e)	2.93%	Section (f)	0.86%
Section (g)	1.29%	Section (h)	0.97%	Section (i)	1.11%

Table 1: The average percentage error of the fabricated lens profile

(a)
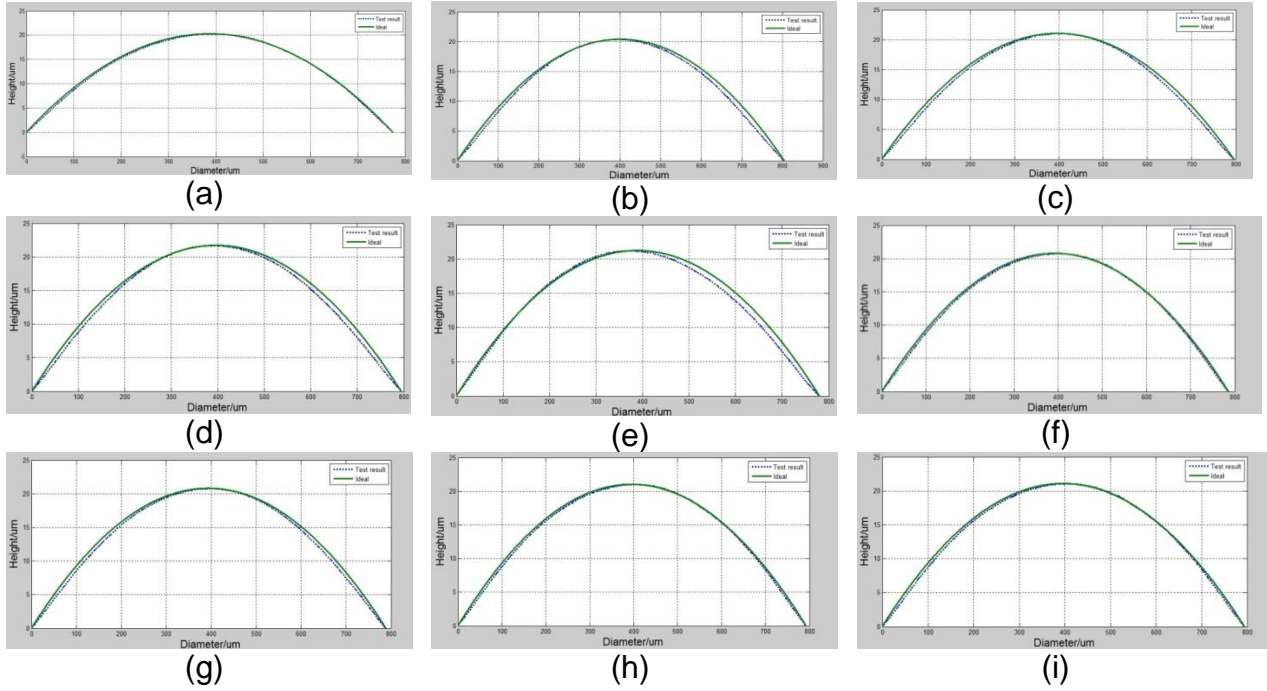
(b)

(c)

(d)

(e)

(f)

(g)

(h)

(i)

Figure 43: A comparison of the fabricated lens profile and the designed profile. A total of nine sections are shown

5. Imaging Tests

After the MSACE is made, a number of imaging tests are conducted. There are three different setups. The first one uses a black-and-white CMOS sensor. The second uses a simple commercial CCD camera. The third one uses an industrial grade CCD camera.

5.1 First setup

The first setup is comprised of a black-and-while CMOS sensor, a lens holding fixture with alignment and focus function, a occlude, and a light source. Test setup is shown in Figure 44.
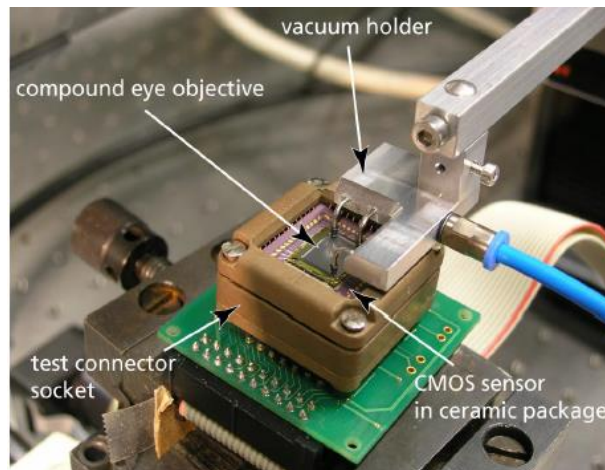

Figure 44: Test platform detail

The test is designed to evaluate the MSACE imaging quality, as well as the effects of different color filters. Although the raw image is black-and-white, by applying

the "Bayer CFA" algorithm, color image can be reconstructed. The basic principle of the algorithm is shown in Figure 46 below.
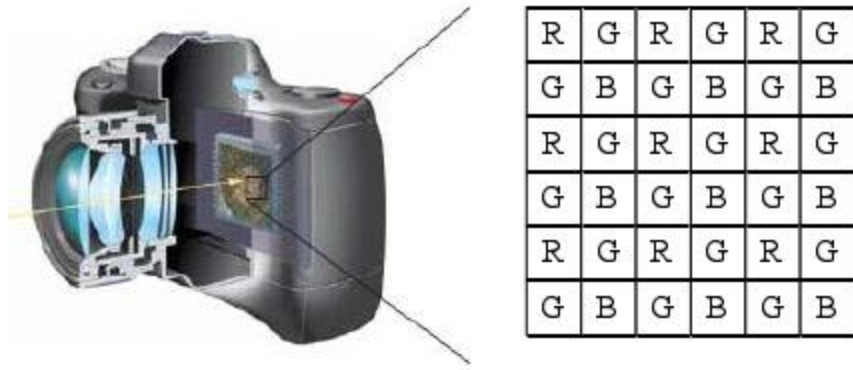

Figure 45: Digital camera and its Bayer CFA

Two cases are tested. Case 1 tests the MSACE made by thermal reflow. Case 2 tests the lens made by injection molding.

Case 1: In this case, the lens is the one shown in Figure 40. The viewing object is a toy magic cube. The testing result is shown in Figure 47. The result figure is a screenshot as the program does not contains a function of output a normal image format, the test program can only output the raw data contains only gray level values. As a result, the image is black-and-white with different gray levels for different color sections, (e.g. the top left hand side is red blue section, the top right hand side is green section, the bottom left hand side is red section, and the bottom right hand side is the infrared pass section).

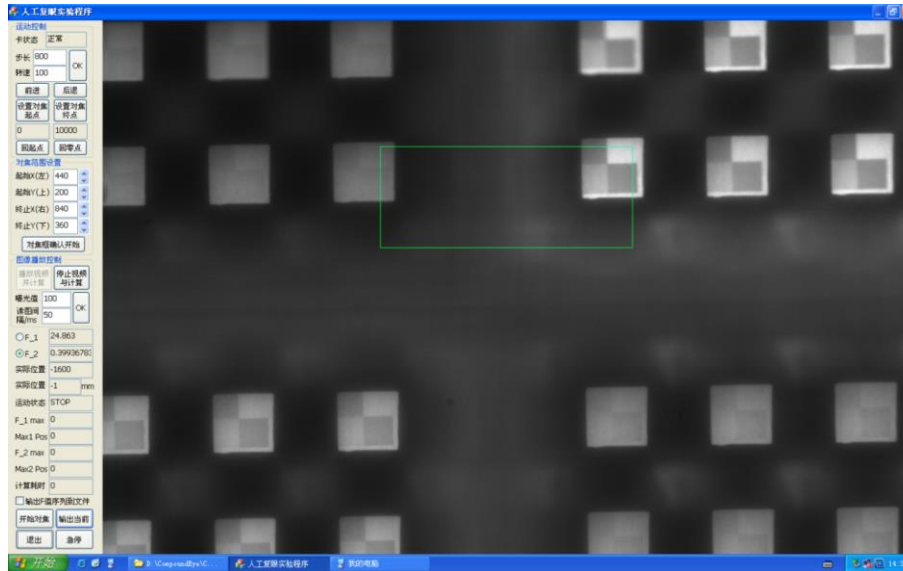Figure 46: The imaging result in Case 1

Case 2: In this case, the lens is fabricated by injection molding as shown in Figures 7 and 8. A 2 X 2 color filter is placed in front of the lens as shown in Figure 48. The imaging result is shown in Figure 49. Comparing to Case 1, the image in Case 2 is sharper.
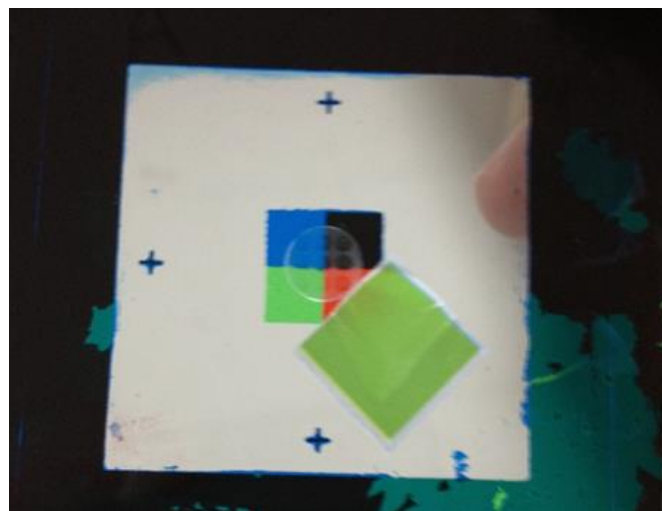
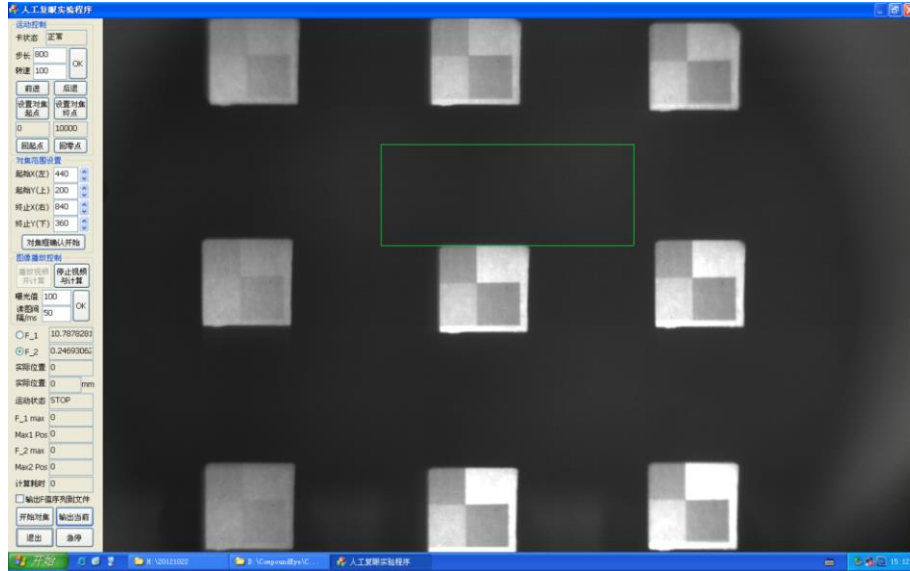Figure 47: The 2 X 2 Multi-spectra filter with custom made lens made by injection molding

Figure 48: The imaging result in Case 2

Figure 50 shows the reconstructed color images using the Bayer CFA algorithm and the normal image. As shown in the figure, the color reconstruction is not very good.
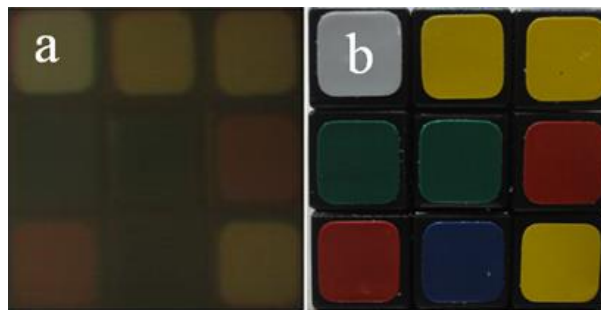
Figure 49: Color reconstruction results of Test setup 1, (a) the reconstructed image of magic cube (b) the image captured by a normal camera

5.2 Second setup

Another method is to use a color CCD sensor. In order to get an color CCD sensor, an old commercial digital camera and two webcam was disassembled, shows in Figure 51 and 52, but none of them was suitable for the image capturing test, the commercial digital camera was very difficult to remove its own lens, it needed to remove all other parts before the lens can be taken out, what's worse, the main board can hardly be removed and when the camera was reassembled, it could not work properly, so this cannot be an option. On the other hand, the CCD sensor of the webcam is too small, only 1/6 inch, and hence, not suitable for the test.
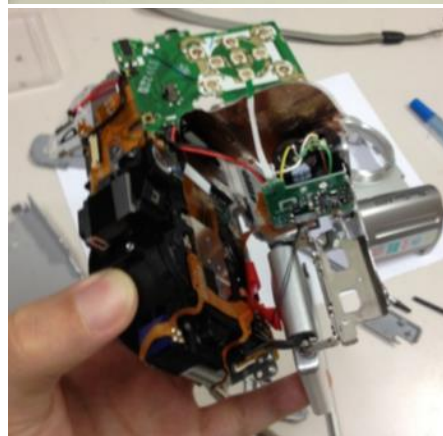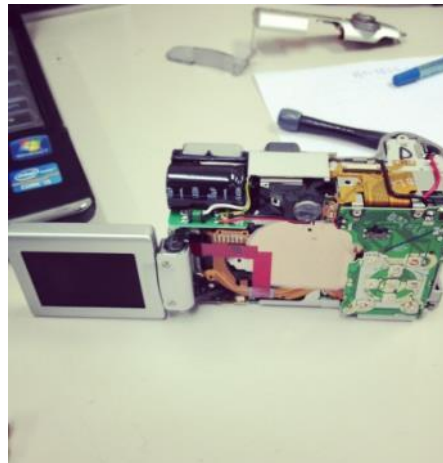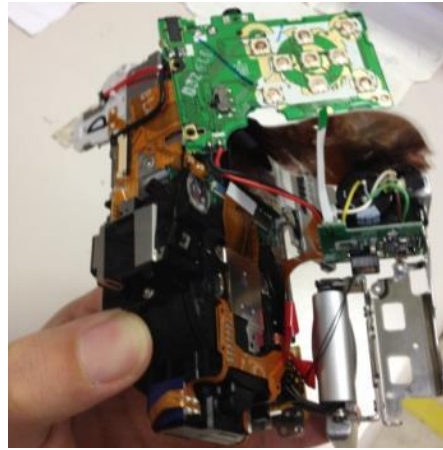
Figure 50: Disassemble a commercial digital camera
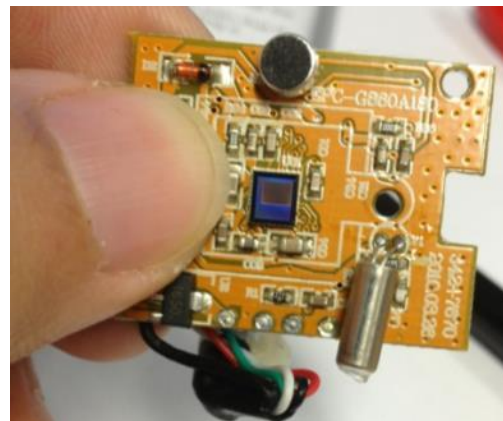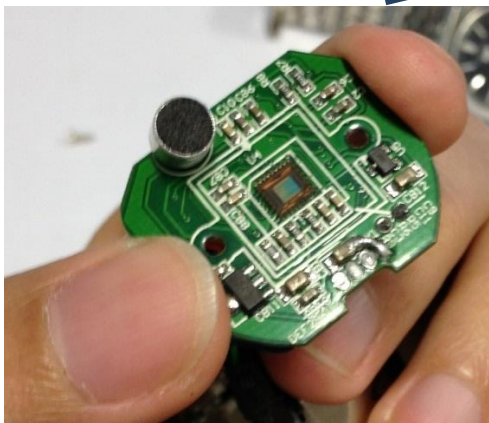
Figure 51: Webcam's CCD sensors are too small for MSACE imaging test

5.3 Third setup

In this setup, an industrial grade CCD sensor (Model: UC1000-C, Manufacturer: Acutance (Beijing) Ltd.) was used. The sensible band of the sensor ranges from 400 nm to 1200 nm. The setup is shown in Figure 53.
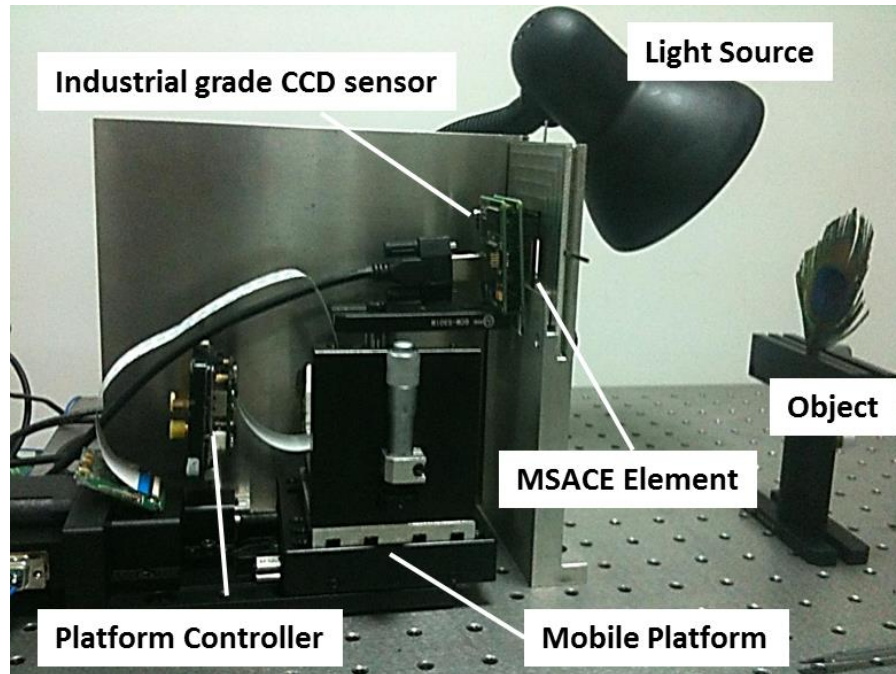
Figure 52: The experiment setup 3 for testing MSACE

Two MSACE systems are tested. One is the 9-color MSACE as shown in Figure 41. It will be referred to as the Sample #1 in the following section. The other uses the ACE made by injection molding method, combine with the multi-spectra filters made by pigment-based photoresist, as shown in the Figure 54. It will be referred to as the Sample #2 in the following section.

Figure 53: Comparison sample, ACE structure made by injection molding + pigment based photoresist multi-spectra filter

When the hardware setup is ready, the software parameters need to be adjusted, so a color magic cube was used as the testing observed object. First turn the magic cube and let one side have as many color as possible (e.g. six), then through the observing software to adjust focus and luminance gain level, etc. The sample adjusted image is shown in Figure 55, it can be clearly see that each section is different from others and most of them are will focused. The sample image provide good enough result, means the setup is qualified for doing the imaging tests, three different observation objects were used: peacock's feather; butterfly and human hand.
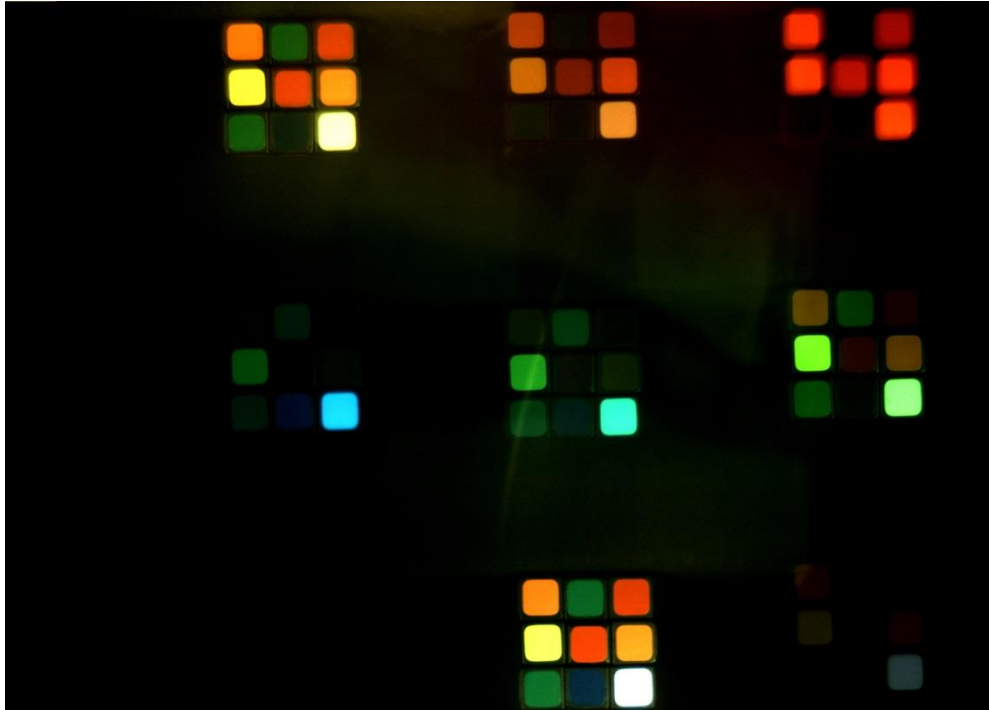
Figure 54: A sample imaging result of the MSACE – magic cube (9 colors)

5.3.1 Imaging test 1

Using the aforementioned setup, the two MSACE samples were first used to take image results of a peacock's feather. Figure 56 shows the original feather, and figure 57 & 58 shows the results from the two samples. The two samples provide similar result: Both of them provide clear, sharp and separated images of the observing object, and each separated image is in different color, moreover, different images show different patterns, for instance, in the red section, the centre pattern and first ring around it has fuzzy boundary, while in the blue and green section, the contrast between the centre pattern and the first ring is very clear; what's more, in the green section, there is a "highlighted" ring near the periphery of the feather pattern, while the same place is not so clear in either red or blue section. This will help to extract the hidden spectral

patterns of the image. The image in the red + green + blue section and violet section are too dark to be seen, that's because the light source using in experiment contents little near infrared and violet light.

Figure 55: Original peacock's feather for observation
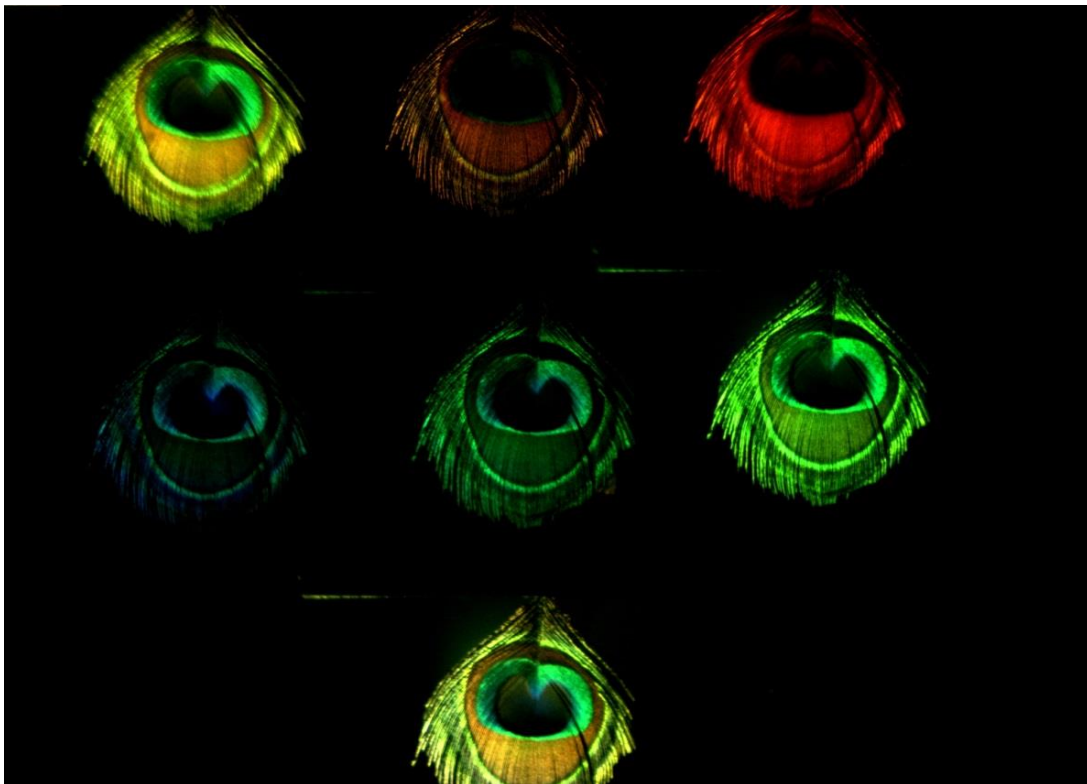
Figure 56: A sample imaging result of the MSACE – peacock's feather (sample #1)
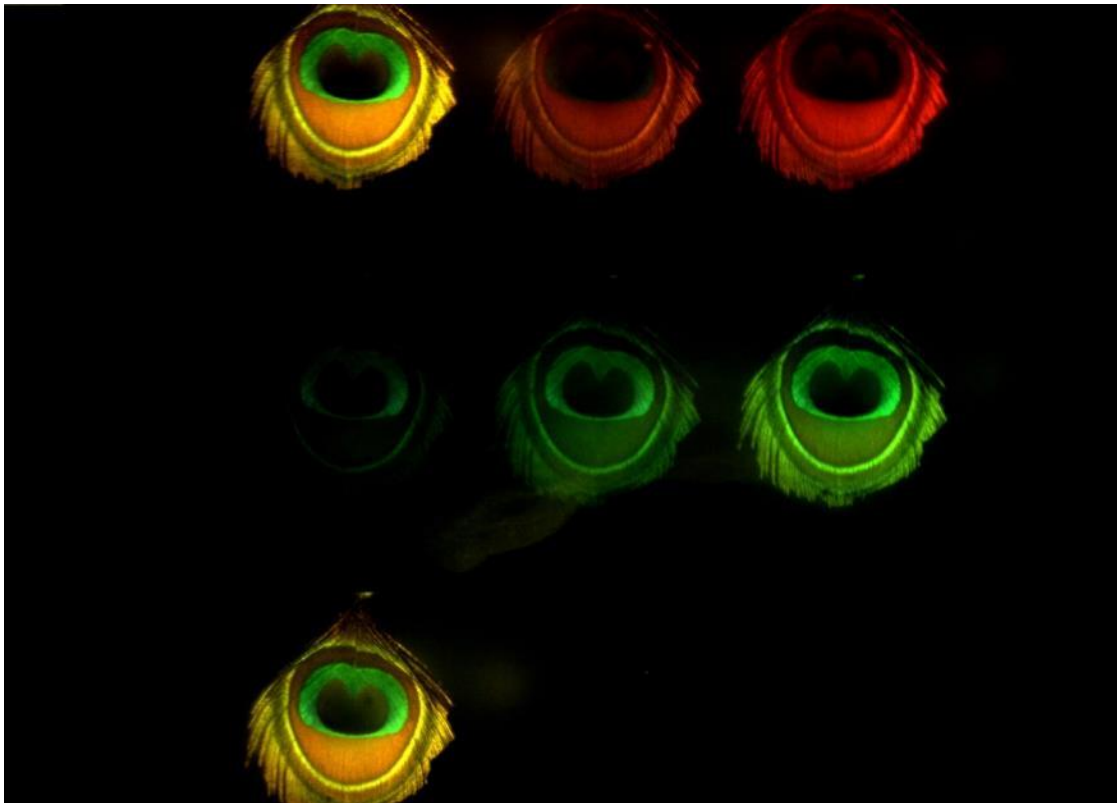
Figure 57: A sample imaging result of the MSACE – peacock's feather (sample #2)

5.3.2 Imaging test 2

Other than using the peacock's feather, some butterflies were also used as observing object, since they have colorful appearance, Figure 59 shows the observed butterfly and Figure 60 & 61 show the testing results of the two samples.

Figure 58: Colorful butterfly specimen for observation

From the two results figures 59 and 60 below, they both show that the originally "write dots" on the butterfly represent in different color in different separate images, and the originally "blue" part on the butterfly only shows in the blue spectra filter image, invisible in other spectra filters; finally the body of the butterfly only reflect yellow light. Since using the same light source as the image test 1, the infrared and violet image are too dart to be seen in the result images.
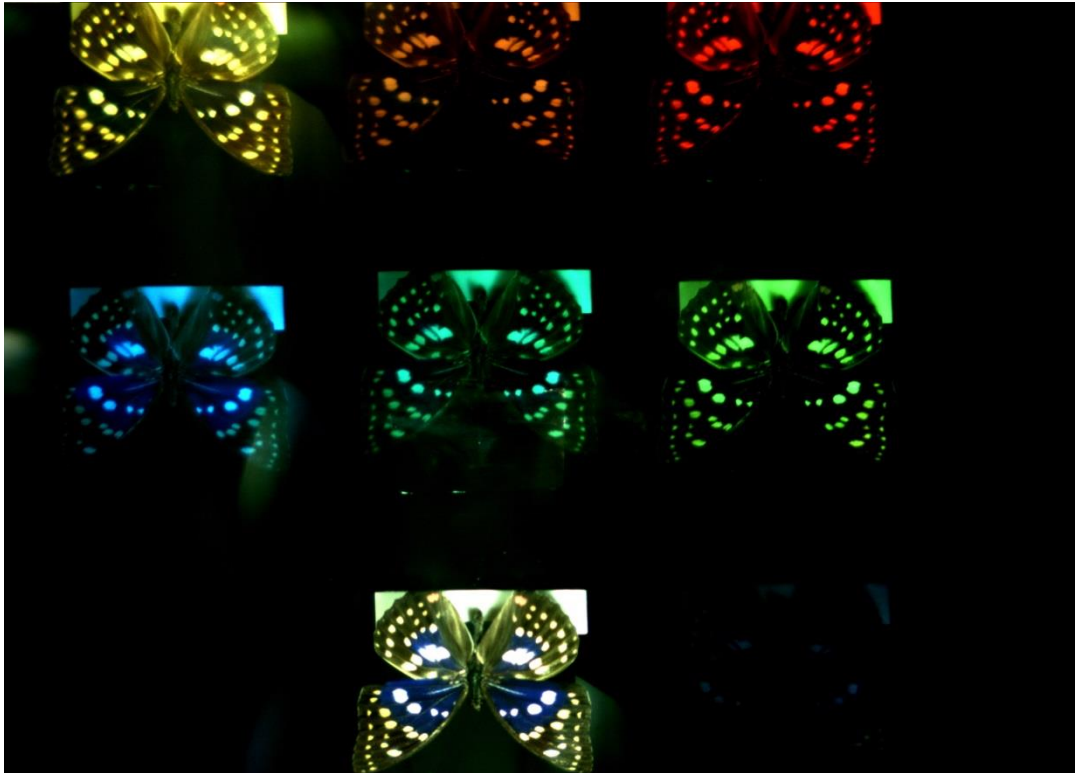
Figure 59: A sample imaging result of the MSACE – butterfly (sample #1)
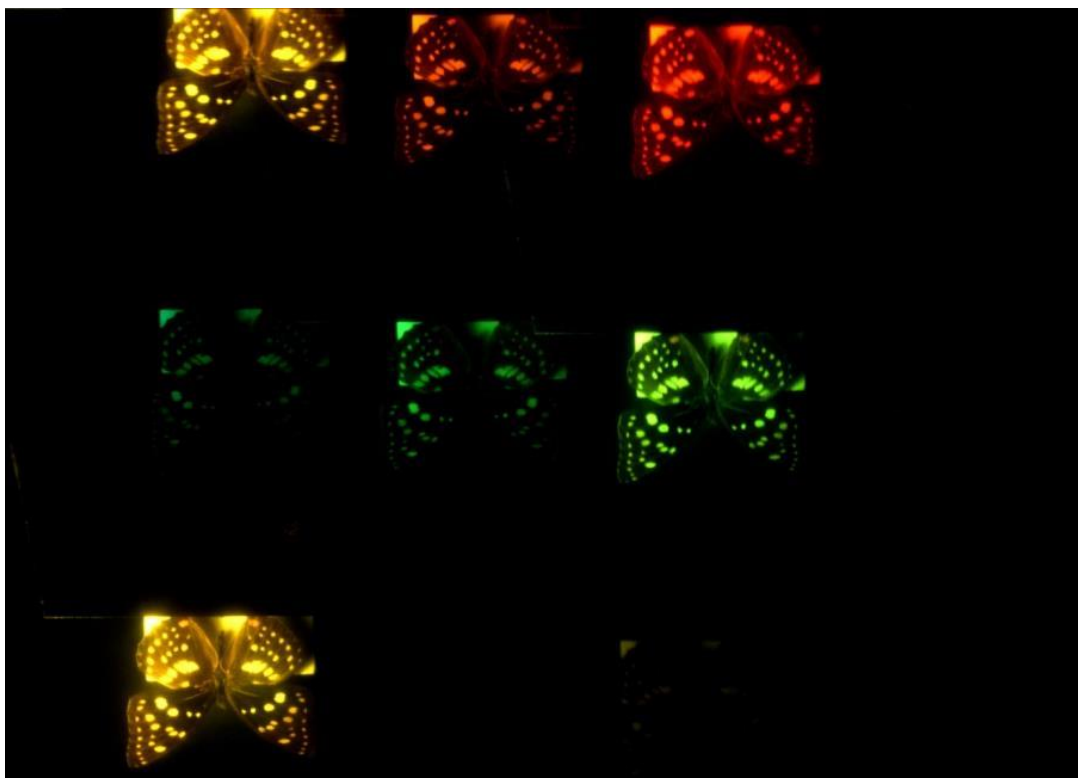
Figure 60: A sample imaging result of the MSACE – butterfly (sample #2)

5.3.3 Imaging test 3

At least, human hand was also put as the observing object, to see if the MSACE can capture some addition information other than the normal lens. Because the observing object shows nearly no different while using the previous light source, as a result, another light source which contents full spectra lights is used in this test. Figure 62 shows the observed human hand, and figure 63 & 64 show the results through two MSACE samples, they show that the veins on human's hand can clearly be seen under MSACE through some spectra filters, especially the orange, cyan, green and violet part, while it normally invisible under normal lighting and normal lens camera. The result clearly shows the advantage of MSACE image system: with the help of specific light source, hidden pattern can be found through the separate images.

Figure 61: Human hands capture by normal camera under fluorescent lighting

Figure 62: A sample imaging result of the MSACE – human hand (Sample #1)
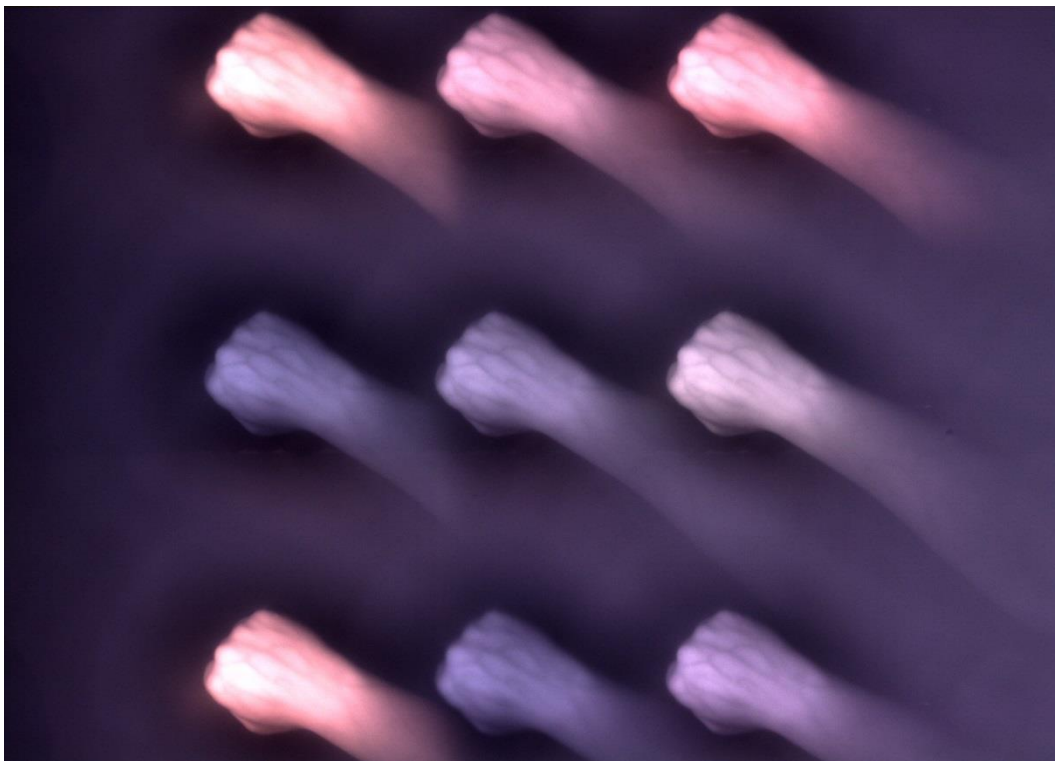
Figure 63: A sample imaging result of the MSACE – human hand (sample #2)

6. Conclusions and Future Work

This thesis presents a novel Multi-Spectra Artificial Compound Eyes (MSACE) system. Based on the discussions above, following conclusions can be drawn:

(1) The process of making multi-spectra filters using pigment-based photoresist is successfully developed.

(2) The process of making MSACE is developed.

(3) The advantages of the MSACE include:

– It can capture different spectra images at the same time;

– It can effectively catch the hidden patterns of an image;

– It is low cost.

It shall be mentioned that the presented MSACE is still in its infancy. From the design point of view, for instance, the micro lens can be in different sizes and shapes, which gives the light field imaging. In addition, many more filters can be added covering more spectral bands. From the fabrication point of view, many improvements can be made, such as applying the heat source on top of the substrate for thermal reflow process other than using a hot plate under the substrate; controlling the thermal reflow temperature and time; using better illuminant in imaging testing, e.g.: lamp of the projector, as the experiment illuminant use in this paper contents little infrared band light, it's expectant that the result can be improved by using better light source.

Bibliography

[1] S. Di, H. Lin and Ruxu Du; "An Artificial Compound Eyes Imaging System Based on MEMS Technology"; Robotics and Biomimetics (ROBIO), 2009 IEEE International Conference

[2] http://en.wikipedia.org/wiki/Eye. access Nov. 2012

[3] http://aph.huji.ac.il/nissimparty/nbackground.htm access Nov. 2012

[4] http://www.lifepixel.com/galleries/uv-ultraviolet-photography-gallery access Nov. 2012

[5] J. Duparre, P. Dannberg, P. Schreiber, A. Brauer and A. Tunnermann, "Artificial apposition compound eye fabricated by micro-optics technology," Appl. Opt., 2004; 43: 4303-4310.

[6] J. Duparre, D. Radtek and A. Tunnermann, "Spherical artificial compound eye captures real images," Proc. SPIE, 2007; 6466: 64660K-1-9.

[7] J. Tanida, T. Kumagai, K. Yamada, S. Miyatake, K. Ishida, T. Morimoto, N. Kondou, D. Miyazaki and Y. Ichioka, "Thin observation module by bound optics (TOMBO): concept and experimental verification," Appl. Opt., 2001; 40: 1806-1813.

[8] R. Shogenji, Y. Kitamura, K. Yamada, S. Miyatake and J. Tanida, "Bimodal fingerprint capturing system based on compound-eye imaging module," Appl. Opt., 2004; 43: 1355-1359.

[9] R. Shogenji, Y. Kitamura, K. Yamada, S. Miyatake and J. Tanida, "Multispectral imaging using compact compound optics," Opt. Express., 2004; 12: 1643-1655.

[10] J. Tanida, R. Shogenji, Y. Kitamura, K. Yamada, M. Miyamoto and S. Miyatake, "Color imaging with an integrated compound imaging system," Opt. Express., 2003; 11: 2109-2117.

[11] R. Horisaki, S. Irie, Y. Ogura and J. Tanida, "Three-dimensional information acquisition using a compound imaging system," Opt. Review., 2007; 14: 347-350.

[12] Z. D. Popovic, R. A. Sprague and G. A. N. Connell, "Technique for monolithic fabrication of microlens array," Appl. Opt., 1988; 27: 1281-1284.

[13] H. Du and M. G. Li, "The study for particle image velocimetry system based on binocular vision," Measurement, 2009; 42: 619-627.

[14] Q. X. Cao, Z. Fu, N. J. Xia and F. L. Lewis, "A binocular machine vision system for ball grid array package inspection," Assembly. Autom., 2005; 25: 217-222.

[15] B.-K. Lee, D. S. Kim, T. H. Kwon; "Replication of microlens arrays by injection

[16] Molding"; Microsystem Technologies October 2004, Volume 10, Issue 6-7, pp 531-535

[17] Z. D. Popvic, R. A. Sprague and G. A. N. Connel, "Technique for monolithic fabrication of microlens arrays," Appl. Opt., vol. 27, no. 7, 1988, pp. 1281-1284.

[18] S. Haselbeck, H. Schreiber, J. Schwider and N. Streibl, "Microlenses fabricated by melting a photoresist on a base layer," Opt. Eng., vol. 32, no. 6, pp. 1322-1324.

[19] William J. Coleman; "Evolution of Optical Thin Films by Sputtering"; APPLIED OPTICS / Vol. 13, No. 4 / April 1974

[20] R. W. Sabnis, "Color Filter Technology for Liquid Crystal Displays," Displays, Vol. 20, pp. 119-129, 1999.

[21] J. Y. Hardeberg, "Multispectral Color Image Capture Using a Liquid Crystal Tunable Filter," Optics Engineering, Vol. 41, No. 10, pp. 2532–2548, October 2002.

[22] http://www.szhlgd.cn/index.asp assess July, 2012

[23] J.M. Zha, "The applications of three symmetry layers in decrease reflect film [J]", Journal of Optical Instrument Technology, 1990, 11(3): 26-31.

[24] John F Rankoeski, "Absorptive band-pass filters for NVIS compatible crew stations". [J]. Proceeding of SPIE, 1986, 2622:38

[25] K. Itoh and O. Matsumoto, "Thin Solid Films" 345, 29 1999.

[26] Z.Y. Ye, D.S. Wang, et al. "Development of Infrared Bandpass Filters with Wide Rejection Band", Journal of Vacuum Science and Technology, 2009, 5: 39

[27] J. Robertson, "Diamond-Like Films and Coatings", NATOASI Series B: Physics, NATO ASI, edited by R. Clausing, L. Horton, J.Angus, and P. Koidl ~Plenum, New York, 1991, pp. 331–356.

[28] G. A. Horridge, "The compound eye of insects," Scientific American, vol. 237, 1977, pp. 108–120.

[29] M. F. Land, "Compound eyes: old and new optical mechanisms," Nature, vol. 287, 1980, pp. 681-686.

[30] S. Ogata, J. Ishida and T. Sasano, "Optical sensor array in an artificial compound eye," Opt. Eng., vol. 34, no. 11, 1994, pp. 3649-3655.

[31] J. S. Sanders and C. E. Halford, "Design and analysis of apposition compound eye optical sensors," Opt. Eng., vol. 34, no. 1, 1995, pp. 222-235.

[32] K. Hamanaka, H. Koshi, "An artificial compound eye using a microlens array and its application to scale invariant processing," Opt. Review., vol. 3, 1996, pp. 264-268.

[33] J. Tanida, Y. Kitamura, K. Yamada, S. Miyatake, M. Miyamoto, T. Morimoto et al., "Compact image capturing system based on compound imaging and digital reconstruction," Proc. SPIE, vol. 4455, 2001, pp. 34-41.

[34] J. Tanida, Y. Kitamura, K. Yamada, S. Miyatake, K. Ishida, T. Morimoto et al., "Thin observation module by bound optics (TOMBO): concept and experimental verification," Appl. Opt., vol. 40, no. 10, 2001, pp. 1806-1813.

[35] J. Duparre, P. Schreiber, P. Dannberg, T. Scharf, P. Pelli, R. Volkel, et al., "Artificial compound eyes – different concepts and their application to ultra flat image acquisition sensors," Proc. SPIE, vol. 5346, 2004, pp. 89-100.

[36] J. Duparre, P. Dannberg, P. Schreiber, A. Brauer and A. Tunnermann, "Artificial apposition compound eye fabricated by micro-optics technology," Appl. Opt., vol. 43, no. 22, 2004, pp. 4303–4310.

[37] J. Duparre, P. Dannberg, P. Schreiber, A. Brauer and A. Tunnermann, "Micro-optically fabricated artificial apposition compound eye," Proc. SPIE, vol. 5301, 2004, pp. 25-33.

[38] Duparre J, Radtke D, Tunnermann A, "Spherical artificial compound eye captures real images," Proc. SPIE, vol. 6466, no. 64660K, 2007, pp. 1-9.

[39] Z. D. Popvic, R. A. Sprague and G. A. N. Connel, "Technique for monolithic fabrication of microlens arrays," Appl. Opt., vol. 27, no. 7, 1988, pp. 1281-1284.

[40] S. Haselbeck, H. Schreiber, J. Schwider and N. Streibl, "Microlenses fabricated by melting a photoresist on a base layer," Opt. Eng., vol. 32, no. 6, pp. 1322-1324.

[41] Gerd E. Keiser. A Review of WDM Technology and Applications. Optical Fiber Technology 5, 3-39 - (1999).

[42] Nahum Gat. Imaging Spectroscopy Using Tunable Filters: A Review. Proc. SPIE Vol. 4056, p. 50-64.

[43] Abbas El Gamal, Helmy Eltoukhy. CMOS image sensors. IEEE CIRCUITS & DEVICES MAGAZINE, May/June 2005.

[44] G. Themelis, J. S. Yoo, V. Ntziachristos. Multispectral imaging using multiple-bandpass filters. OPTICS LETTERS, May 1, 2008 / Vol. 33, No. 9.

[45] Jason M. Eichenholz .Real time Megapixel Multispectral Bioimaging. SPIE Proceeding, Vol., 7568, p.75681L, (2010)

[46] Hongfei Jiao, Yonggang Wu. Two-chamber integrated multichannel narrowband filter

[47] prepared by a multistep etching method. APPLIED OPTICS, 20 February 2007, Vol. 46, No. 6

[48] Ram W. Sabnis. Color filter technology for liquid crystal displays. Displays 20 (1999) 119–129.

[49] G. Themelis, J. S. Yoo, and V. Ntziachristos, "Multispectral Imaging Using Multiple-Bandpass Filters," Optics Letters, Vol. 33, No. 9, 2008.

[50] J. M. Eichenholz, N. Barnett, and et al, "Real Time Megapixel Multispectral Bioimaging," Proc. of SPIE, Paper No. 7568, Jan. 2010.

Appendix A: Publications during my studies

- Y.P. Yao, R. Du, "Multi-Spectra Artificial Compound Eyes, Design, Fabrication and Applications", Proceedings of the 2013 World Congress in Computer Science, Computer Engineering, and Applied Computing, July 22-25, 2013, Las Vegas, USA
- J. Jin, S. Di, Y.P. Yao, "Design and fabrication of filtering artificial-compound-eye and its application in multi-spectral imaging", Proc. SPIE, 2013
- J. Jin, S. Di, Y.P. Yao, "Design and fabrication of an integrated multi-channel optical filter working in visible and near-infrared bands", Applied Mechanics and Materials Vol. 289 (2013) pp 63-68

Appendix B: Matlab® codes of testing photoresist lens surface profile.

This program compares the thermal reflow lens surface profile and the ideal sphere surface profile.

```
clear

Limit=3.0;
global RawData

%function ReadData()

[FileName,PathName]=uigetfile('*.dat');
%tic
%FileName='D:\Documents\Matlab\ContourDataAnalysis\RawData\C2.2-21.dat';
Routine=[PathName FileName];
RawData_temp=importdata(Routine,',',6);       %µ¼ÈëµÄÇ¸ö½á¹¹Ìå
RawData=RawData_temp.data;                      %°Ñ½á¹¹ÌåÖÐµÄÊý¾Ý´æÎªÔ-Ê¼Êý¾Ý
clear RawData_temp;                             %Çå¿ÕÁÙÊ±µÄ½á¹¹Ìå
RawLength=length(RawData);
LowerLimNum=0;
UpperLimNum=RawLength;

for x=1:1:RawLength;
    if RawData(x,2)>Limit
        LowerLimNum=x;
        break
    end
end

for y=RawLength:-1:1;
    if RawData(y,2)>Limit
        UpperLimNum=y;
        break
    end
end

ProcessData=RawData(LowerLimNum:UpperLimNum,:);


DisplayActualData=ProcessData;
DisplayActualData(:,1)=ProcessData(:,1)-ProcessData(1,1);
DisplayActualData(:,2)=ProcessData(:,2)-Limit;

Diameter=DisplayActualData(end,1)-DisplayActualData(1,1);
Height=max(DisplayActualData(:,2));   %%%%%%%%%%½«ÀíÂÛÐÎ×´µÄ¸ß¶È»Ö¸´ÖÁÄ¬ÈÏ
Radius=(Diameter^2+4*Height^2)/8/Height;

DisplayTheoricalData(:,1)=DisplayActualData(:,1);
TheoricalData_temp=(Radius^2-(DisplayTheoricalData(:,1)-Diameter/2).^2).^0.5;
DisplayTheoricalData(:,2)=TheoricalData_temp-min(TheoricalData_temp);
```
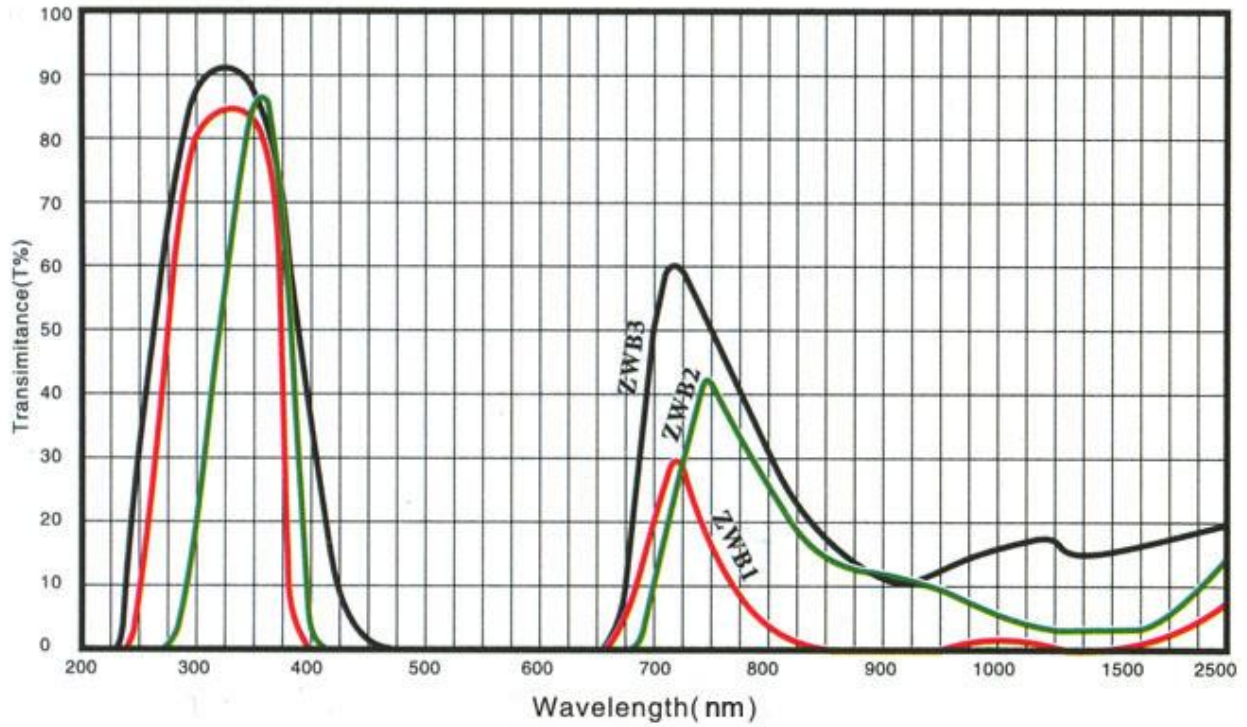
```matlab
p=plot(DisplayActualData(:,1),DisplayActualData(:,2),':',DisplayTheoricalData
(:,1),DisplayTheoricalData(:,2));
%p=plot(DisplayActualData(:,1),DisplayActualData(:,2),':');
grid on;

xlabel('Diameter/um','FontSize',16);
ylabel('Height/um','FontSize',16);
set(p(1),'LineWidth',2.5);
set(p(2),'LineWidth',2.5);
legend('Test result','Ideal');
hold on;
```
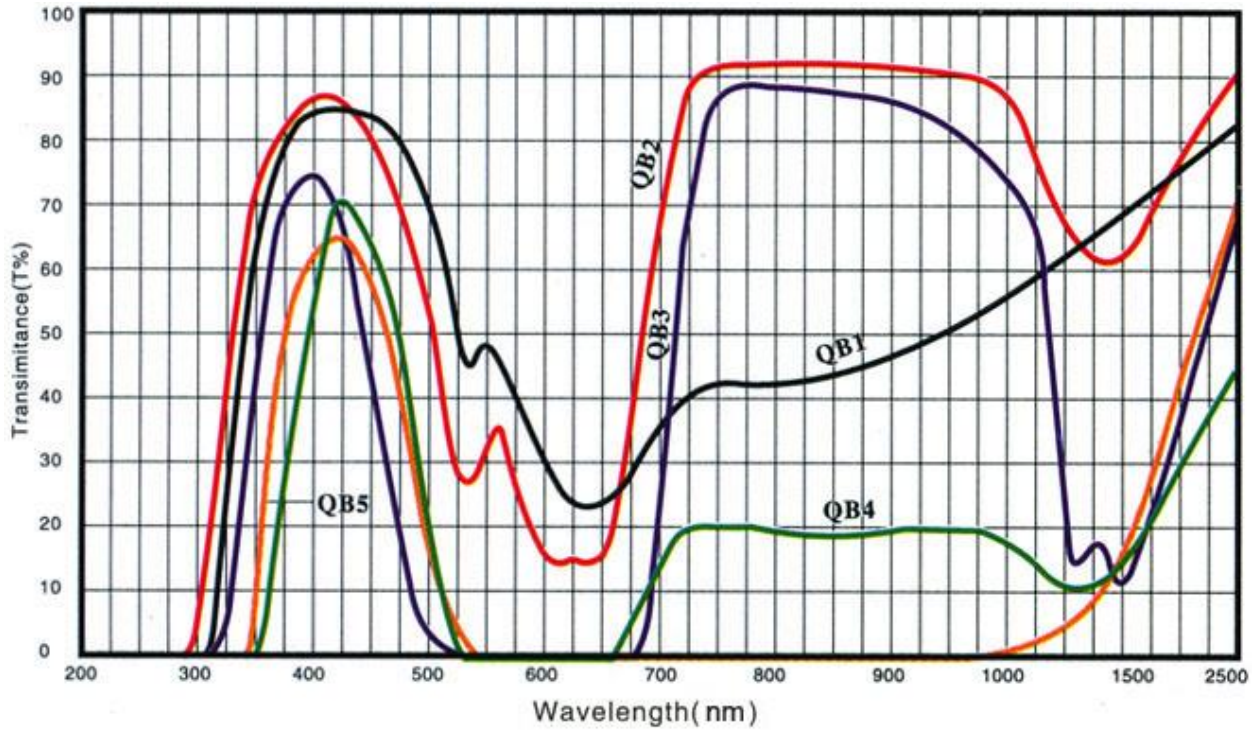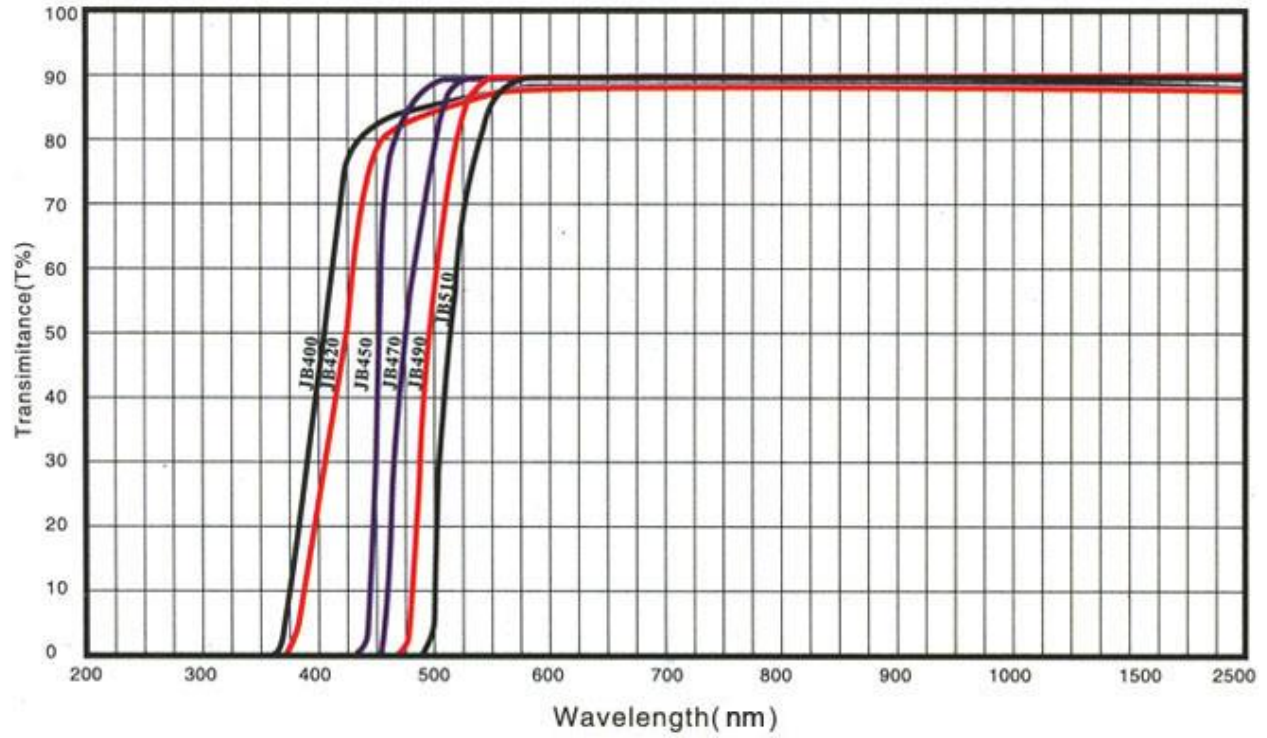
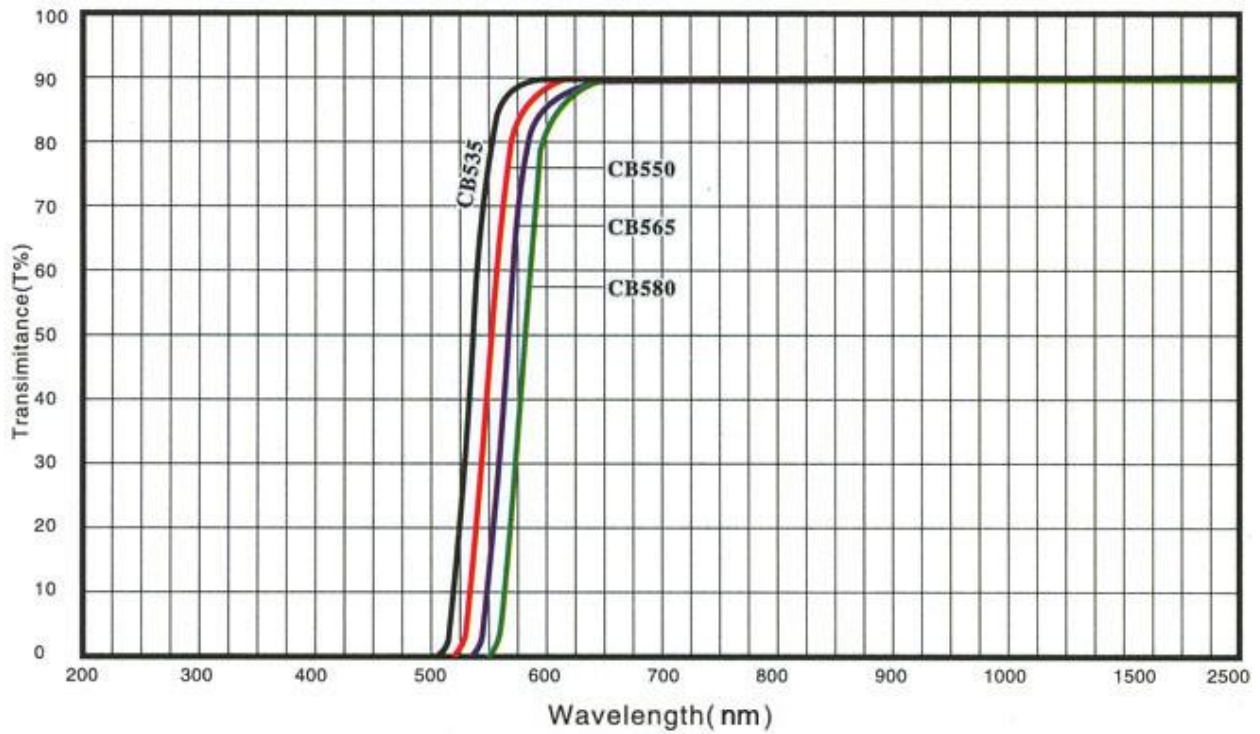**Appendix C: Transmittance of purchased color filters**

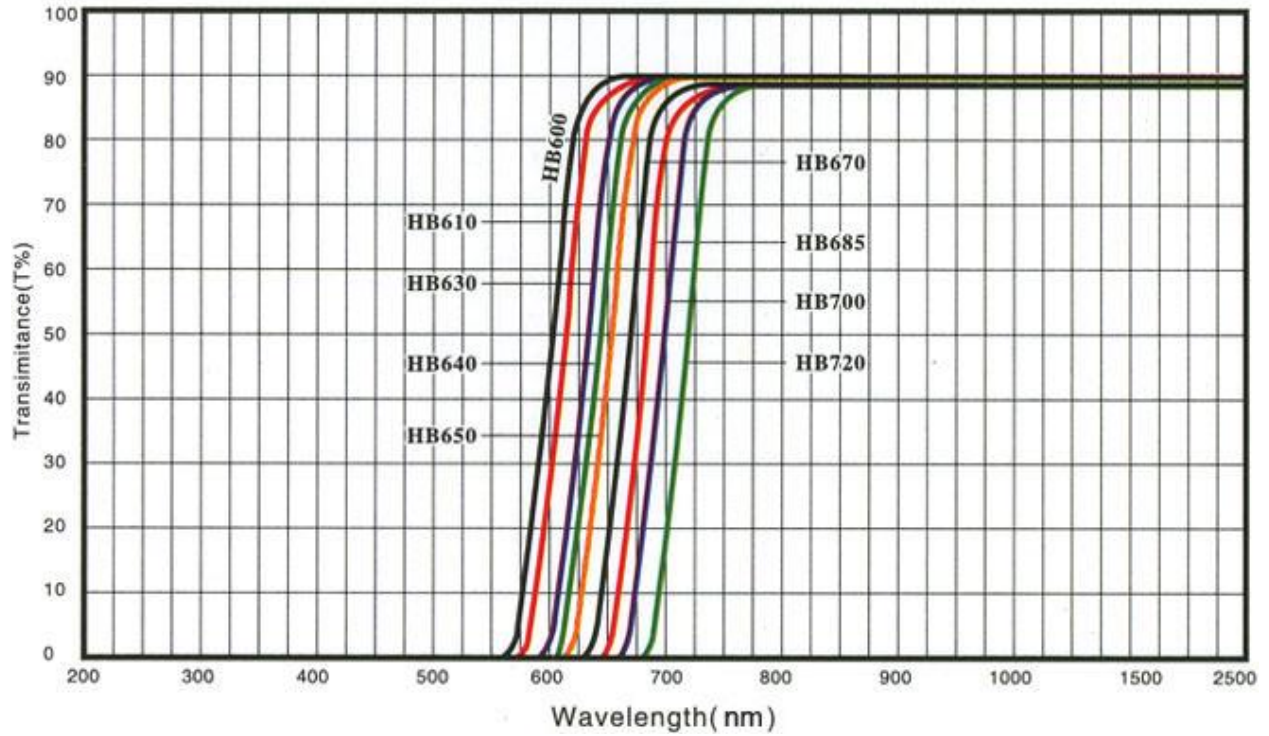ZWB1 ZWB2 UV pass glass filter spectra specification
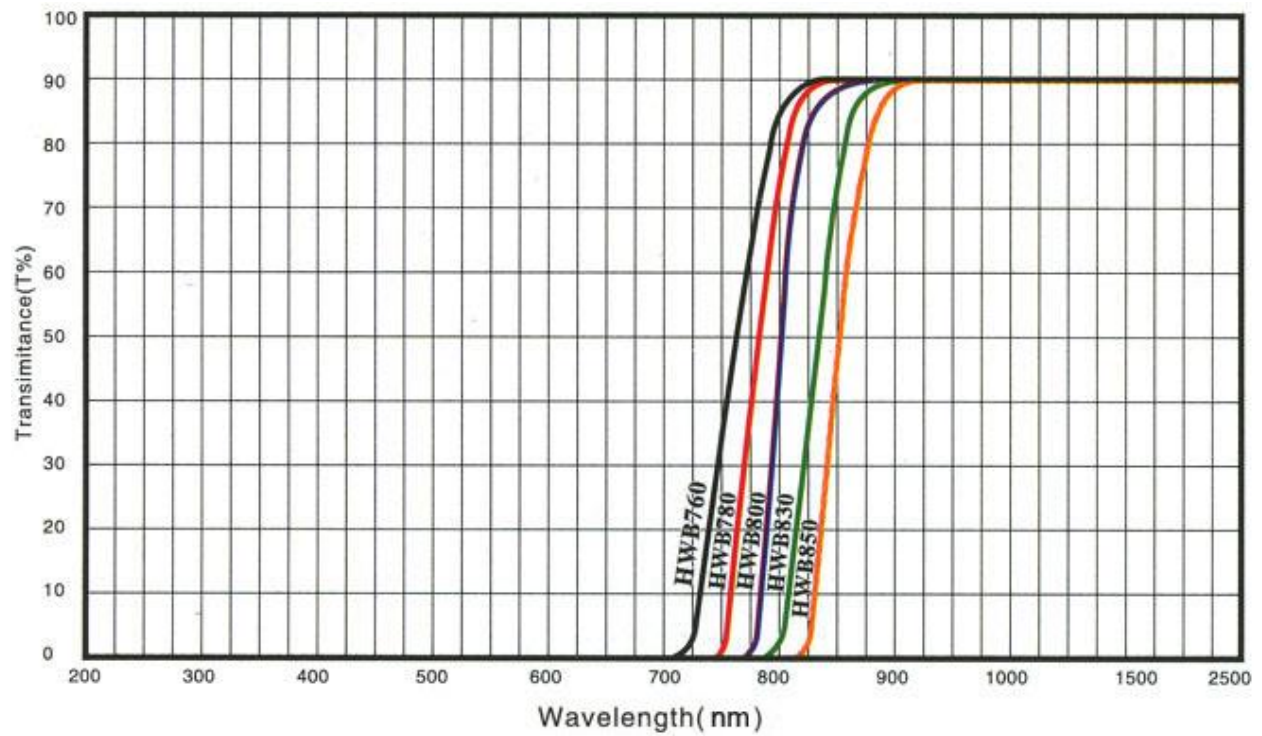

QB1 QB4 blue pass filter spectra specification

JB 470 Yellow (green) glass filter spectra specification

CB 535 Orange glass filter spectra specification

HB 630 HB700 Red glass filter spectra specification

HWB 830 Infrared pass glass filter spectra specification